OXFORD

Les Houches 2014

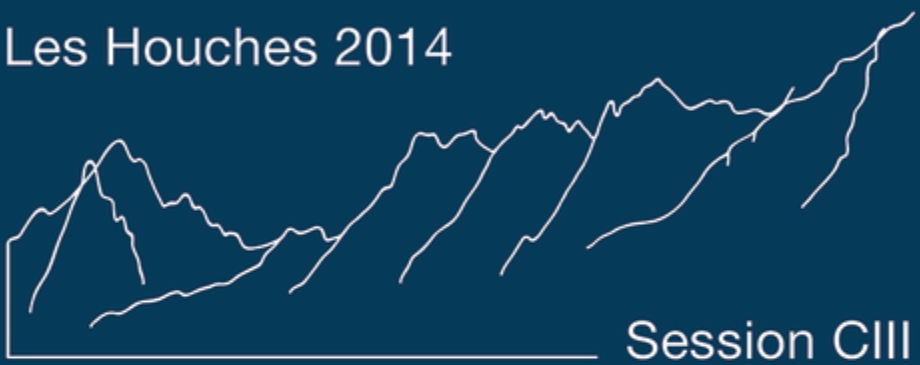

Session CIII

Topological Aspects of Condensed Matter Physics

C. Chamon
M. O. Goerbig
R. Moessner
L. F. Cugliandolo

Editors

Topological Aspects of Condensed Matter Physics

École de Physique des Houches

Session CIII, 4–29 August 2014

Topological Aspects of Condensed Matter Physics

Edited by

Claudio Chamon

Physics Department, Boston University, Boston, Massachusetts, 02215, USA

Mark O. Goerbig

Laboratoire de Physique des Solides, CNRS UMR 8502, Université Paris-Sud,Université Paris-Saclay F-91405, France

Roderich Moessner

Max-Planck-Institut für Physik komplexer Systeme, 01187 Dresden, Germany

Leticia F. Cugliandolo

Sorbornne Universités, Université Pierre et Marie Curie, Laboratoire de Physique Théorique et Hautes Energies, CNRS UMR 7589, Paris, France

OXFORD
UNIVERSITY PRESS

OXFORD
UNIVERSITY PRESS

Great Clarendon Street, Oxford, OX2 6DP,
United Kingdom

Oxford University Press is a department of the University of Oxford.
It furthers the University's objective of excellence in research, scholarship,
and education by publishing worldwide. Oxford is a registered trade mark of
Oxford University Press in the UK and in certain other countries

First Edition published in 2017

Impression: 1

Published in the United States of America by Oxford University Press
198 Madison Avenue, New York, NY 10016, United States of America

British Library Cataloguing in Publication Data
Data available

Library of Congress Control Number: 2016943652

ISBN 978–0–19–878578–1

Printed and bound by
CPI Group (UK) Ltd, Croydon, CR0 4YY

École de Physique des Houches

Service inter-universitaire commun
à l'Université Joseph Fourier de Grenoble
et à l'Institut National Polytechnique de Grenoble

Subventionné par l'Université Joseph Fourier de Grenoble,
le Centre National de la Recherche Scientifique,
le Commissariat à l'Énergie Atomique

Directeur:
Leticia F. Cugliandolo, Sorbonne Universités, Université Pierre et Marie Curie
Laboratoire de Physicque Théorique et Hautes Energies, Paris, France

Directeurs scientifiques de la session:
Claudio Chamon, Physics Department, Boston University, Boston, Massachusetts, USA
Mark O. Goerbig, Laboratoire de Physique des Solides, CNRS UMR 8502, Université Paris-Sud, France
Roderich Moessner, Max-Planck-Institut für Physik komplexer Systeme, Dresden, Germany
Leticia F. Cugliandolo, Sorbornne Universités, Université Pierre et Marie Curie, Laboratoire de Physique Thèorique et Hautes Energies, Paris, France

Previous Sessions

I	1951	Quantum mechanics. Quantum field theory
II	1952	Quantum mechanics. Statistical mechanics. Nuclear physics
III	1953	Quantum mechanics. Solid state physics. Statistical mechanics. Elementary particle physics
IV	1954	Quantum mechanics. Collision theory. Nucleon-nucleon interaction. Quantum electrodynamics
V	1955	Quantum mechanics. Non equilibrium phenomena. Nuclear reactions. Interaction of a nucleus with atomic and molecular fields
VI	1956	Quantum perturbation theory. Low temperature physics. Quantum theory of solids. Ferromagnetism
VII	1957	Scattering theory. Recent developments in field theory. Nuclear and strong interactions. Experiments in high energy physics
VIII	1958	The many body problem
IX	1959	The theory of neutral and ionized gases
X	1960	Elementary particles and dispersion relations
XI	1961	Low temperature physics
XII	1962	Geophysics; the earths environment
XIII	1963	Relativity groups and topology
XIV	1964	Quantum optics and electronics
XV	1965	High energy physics
XVI	1966	High energy astrophysics
XVII	1967	Many body physics
XVIII	1968	Nuclear physics
XIX	1969	Physical problems in biological systems
XX	1970	Statistical mechanics and quantum field theory
XXI	1971	Particle physics
XXII	1972	Plasma physics
XXIII	1972	Black holes
XXIV	1973	Fluids dynamics
XXV	1973	Molecular fluids
XXVI	1974	Atomic and molecular physics and the interstellar matter
XXVII	1975	Frontiers in laser spectroscopy
XXVIII	1975	Methods in field theory
XXIX	1976	Weak and electromagnetic interactions at high energy
XXX	1977	Nuclear physics with heavy ions and mesons

XXXI	1978	Ill condensed matter
XXXII	1979	Membranes and intercellular communication
XXXIII	1979	Physical cosmology
XXXIV	1980	Laser plasma interaction
XXXV	1980	Physics of defects
XXXVI	1981	Chaotic behavior of deterministic systems
XXXVII	1981	Gauge theories in high energy physics
XXXVIII	1982	New trends in atomic physics
XXXIX	1982	Recent advances in field theory and statistical mechanics
XL	1983	Relativity, groups and topology
XLI	1983	Birth and infancy of stars
XLII	1984	Cellular and molecular aspects of developmental biology
XLIII	1984	Critical phenomena, random systems, gauge theories
XLIV	1985	Architecture of fundamental interactions at short distances
XLV	1985	Signal processing
XLVI	1986	Chance and matter
XLVII	1986	Astrophysical fluid dynamics
XLVIII	1988	Liquids at interfaces
XLIX	1988	Fields, strings and critical phenomena
L	1988	Oceanographic and geophysical tomography
LI	1989	Liquids, freezing and glass transition
LII	1989	Chaos and quantum physics
LIII	1990	Fundamental systems in quantum optics
LIV	1990	Supernovae
LV	1991	Particles in the nineties
LVI	1991	Strongly interacting fermions and high Tc superconductivity
LVII	1992	Gravitation and quantizations
LVIII	1992	Progress in picture processing
LIX	1993	Computational fluid dynamics
LX	1993	Cosmology and large scale structure
LXI	1994	Mesoscopic quantum physics
LXII	1994	Fluctuating geometries in statistical mechanics and quantum field theory
LXIII	1995	Quantum fluctuations
LXIV	1995	Quantum symmetries
LXV	1996	From cell to brain
LXVI	1996	Trends in nuclear physics, 100 years later
LXVII	1997	Modeling the earths climate and its variability
LXVIII	1997	Probing the Standard Model of particle interactions
LXIX	1998	Topological aspects of low dimensional systems
LXX	1998	Infrared space astronomy, today and tomorrow
LXXI	1999	The primordial universe

LXXII	1999	Coherent atomic matter waves
LXXIII	2000	Atomic clusters and nanoparticles
LXXIV	2000	New trends in turbulence
LXXV	2001	Physics of bio-molecules and cells
LXXVI	2001	Unity from duality: Gravity, gauge theory and strings
LXXVII	2002	Slow relaxations and nonequilibrium dynamics in condensed matter
LXXVIII	2002	Accretion discs, jets and high energy phenomena in astrophysics
LXXIX	2003	Quantum entanglement and information processing
LXXX	2003	Methods and models in neurophysics
LXXXI	2004	Nanophysics: Coherence and transport
LXXXII	2004	Multiple aspects of DNA and RNA
LXXXIII	2005	Mathematical statistical physics
LXXXIV	2005	Particle physics beyond the Standard Model
LXXXV	2006	Complex systems
LXXXVI	2006	Particle physics and cosmology: the fabric of spacetime
LXXXVII	2007	String theory and the real world: from particle physics to astrophysics
LXXXVIII	2007	Dynamos
LXXXIX	2008	Exact methods in low-dimensional statistical physics and quantum computing
XC	2008	Long-range interacting systems
XCI	2009	Ultracold gases and quantum information
XCII	2009	New trends in the physics and mechanics of biological systems
XCIII	2009	Modern perspectives in lattice QCD: quantum field theory and high performance computing
XCIV	2010	Many-body physics with ultra-cold gases
XCV	2010	Quantum theory from small to large scales
XCVI	2011	Quantum machines: measurement control of engineered quantum systems
XCVII	2011	Theoretical physics to face the challenge of LHC
Special Issue	2012	Advanced data assimilation for geosciences
XCVIII	2012	Soft interfaces
XCIX	2012	Strongly interacting quantum systems out of equilibrium
C	2013	Post-Planck cosmology
CI	2013	Quantum Optics and Nanophotonics
Special Issue		Statistical Physics, Optimization, Inference and Message-Passing Algoritms

Publishers

– Session VIII: Dunod, Wiley, Methuen
– Sessions IX and X: Herman, Wiley
– Session XI: Gordon and Breach, Presses Universitaires
– Sessions XII–XXV: Gordon and Breach
– Sessions XXVI–LXVIII: North Holland
– Session LXIX–LXXVIII: EDP Sciences, Springer
– Session LXXIX–LXXXVIII: Elsevier
– Session LXXXIX– : Oxford University Press

Preface

Topological condensed matter physics is a recent arrival among the disciplines of modern physics, with a distinctive and substantive nature. Its roots, however, reach far back, to Dirac's magnetic monopoles and strings of the early 1930s and Skyrme's topologically non-trivial solutions in the nonlinear sigma models of nuclear physics of the 1960s. In the 1970s, the influx of topology into physics came in parallel in different subdisciplines: mathematical physics, high-energy physics, and condensed matter physics.

Much of the current importance of topological condensed matter physics derives from exciting developments in the last half-century. These include, in the 1970s, Wegner's farsighted analysis of lattice gauge theories and the foundation of the study of what is now known as order beyond the Landau–Ginzburg–Wilson paradigm; the work of Kosterlitz and Thouless on the eponymous phase; Anderson's pioneering work on an alternative type of magnetic state of matter, the resonating valence bond liquids; and the seminal studies by Jackiw and Rebbi and by Su, Schrieffer, and Heeger of solitons and topological zero modes with concomitant charge fractionalization in one-dimensional systems.

In the 1980s, there was an outburst of developments in which topology took centre stage in condensed matter physics, many inspired by the experimental discovery of the integer quantum Hall effect by von Klitzing and of the fractional effect by Tsui, Störmer, and Gossard. This was the time when the foundational concepts of Berry's phase and Thouless's pumps arose, when Haldane added a topological term to field theories of spin chains, and when Laughlin's work on the fractional quantum Hall effect lifted charge fractionalization to two-spatial dimensions and provided a setting where anyon statistics could appear. The fractional quantum Hall effect also opened the door for topological field theories to enter condensed matter physics, along with protected edge states and the notion of topological order. These concepts and their relation with quantum Hall physics were at the centre of an earlier Les Houches school, 'Topological Aspects of Low-Dimensional Systems', organized in 1998.

The field has since advanced rapidly, grown explosively, and diversified greatly. We now have a zoo of topological phenomena—the quantum spin Hall effect, topological insulators, Coulomb spin liquids, and non-Abelian anyonic statistics and their potential application in topological quantum computing, to name but a few—as well as an increasingly sophisticated set of concepts and methods underpinning their understanding.

Our aim for this Les Houches Summer School was to present an overview of this field, along with a sense of its origins and its place on the map of advances in fundamental physics. The school comprised a set of basic lectures (Part 1) aimed at a pedagogical introduction of the fundamental concepts, together with more advanced

lectures (Part 2) covering individual topics at the forefront of today's research in condensed matter physics.

This school was, to its date, the most sought after of the Les Houches Schools in terms of number of applicants, which we read as evidence of the interest and relevance of the topic to modern condensed matter physics. Its popularity forced us to reject such a large number of suitable applicants that we decided to video-record the lectures, which can now be viewed at the school's website http://topo-houches.pks.mpg.de.

We thus hope that this book, along with these video recordings, will provide access to the knowledge shared at the school to audiences from all corners of the globe—an earnest way to express our intentions, even if geometrically imprecise!

The book starts with two conceptual presentations, by J. Moore and by B. A. Bernevig (with T. Neupert). The former introduces topological band theory, topological field theories, and Berry phases. The latter introduces the concepts of topological superconductivity and of fractional excitations along with their description within the framework of category theory. These are followed by the lecture notes of J. Chalker, which are oriented towards spin systems, more specifically spin liquids and frustrated magnetism.

The physics of the quantum Hall effect, which may be viewed as a paradigm of topological condensed matter physics, was covered in several advanced lectures. A modern view of the quantum Hall effect is provided by N. Regnault, within the framework of entanglement spectra and advanced numerical techniques. Historical and experimental aspects of this field were covered in a short series of seminars by K. von Klitzing, which, along with other experimental seminars, are available in video form on the school's website (http://topo-houches.pks.mpg.de).

The second part of the book is concerned with the advanced and more specialized lectures. F. Wegner's presentation provides a broad view on lattice gauge theories, harking back to the very origins of the field in the duality construction of phase transitions not associated with a local order parameter.

Generalizations of topological insulators due to interaction effects are the topic of A. Vishwanath's contribution. The topological tenfold-way classification of insulators and superconductors, as well as a stability analysis of one-dimensional edge channels at the boundary of two-dimensional Abelian topological phases, are presented by C. Mudry, who also gives an introduction to Abelian bosonization.

One-dimensional lattice systems are covered by F. Pollmann's lecture notes, where state-of-the art numerical techniques are introduced, such as matrix product states and their descendants. To conclude the study of one-dimensional topological systems, F. von Oppen expands on the topic of topological superconductivity in quantum wires and quantum chains.

The lecture notes by D. Carpentier are concerned with the transport properties of the $(D-1)$-dimensional surface states that accompany many topological phases living in D dimensions. A particular aspect of quantum Hall systems, namely quantum Hall ferromagnetism and its charged topological spin textures, skyrmions, is presented within the context of a modern approach by B. Douçot.

C. Castelnovo covers out-of-equilibrium properties in spin systems and kinetically constrained models. The topical lectures conclude with those by A. Niemi on topology and the physics of proteins and their folding.

All in all, we felt an acute need for a written account of the state of the field, much of the introductory material on which is scattered among review articles in the literature. The lecture notes collated in this volume, along with their oral deliveries, hopefully present a reasonably complete and concise introduction to the burgeoning field of topological condensed matter physics.

The school and the realization of this book would not have been possible without generous financial support from the continuous-formation programme 'École thématique' of CNRS and from the Franco-German University (DFH-UFA). Financial support from the European Spallation Source should also be acknowledged. We would furthermore like to thank all the participants—lecturers and students—for their stimulating interactions and scientific discussions, the outcome of which is also reflected in the present lecture notes. These interactions were favoured by the extremely pleasant environment of the Physics Centre at Les Houches, and we would therefore also like to acknowledge its administrative staff. Finally, we would like to most warmly thank Titus Neupert for the portraits of the various speakers, which figure at the beginning of their respective lecture notes.

As we were finalising these lecture notes for publication, the Nobel Prize 2016 was awarded to Duncan Haldane, Michael Kosterlitz and David Thouless "for theoretical discoveries of topological phase transitions and topological phases of matter", and the Buckley Prize 2017 of the American Physical Society to Alexei Kitaev and Xiao-gang Wen "for theories of topological order and its consequences in a broad range of physical systems". We hope that this recognition will further motivate students of all ages to learn about, and start contributing to, this exciting field of physics.

Claudio Chamon,
Mark O. Goerbig,
Roderich Moessner,
Leticia F. Cugliandolo


Hard Rock
CAFE


ÉCOLE DE
PHYSIQUE
HOUCHES

Contents

List of Participants

Organizers

CHAMON Claudio
Boston University, USA

GOERBIG Mark-Oliver
CNRS Université Paris Sud, Orsay, France

MOESSNER Roderich
Max Planck Institute, Dresden, Germany

Lecturers

BERNEVIG Andrei
Princeton University, USA

CARPENTIER David
CNRS ENS, Lyon, France

CASTELNOVO Claudio
University of Cambridge, UK

CHALKER John T.
University of Oxford, UK

DIL Hugo
PSI and EPFL, Lausanne, Switzerland

DOUCOT Benoît
CNRS Université Pierre et Marie Curie, Paris, France

GAULIN Bruce
McMaster University, Hamilton, Canada

KIM Philip
Columbia University, New York, USA

LEVITOV Leonid
MIT, Cambridge, USA

MOLENKAMP Laurens
Würzburg University, Germany

MOORE Joel
University of California Berkeley, USA

MUDRY Christopher
Paul Scherrer Institute, Villengen, Switzerland

NIEMI Antti
Uppsala University, Sweden

POLLMANN Frank
Max Planck Institute, Dresden, Germany

REGNAULT Nicolas
CNRS ENS, Paris, France; Princeton University, USA

STERN Ady
Weizmann Institute Rehovot Israel

TAKAGI Hidenori
Max Planck Institute, Stuttgart, Germany

VISHWANATH Ashvin
University of California Berkeley, USA

VON KLITZING Klaus
Max Planck Institute Stuttgart, Germany

VON OPPEN Felix
Freie Universität Berlin, Germany

WEGNER Franz
Heidelberg University, Germany

WEN Xiao-Gang
MIT, Cambridge, USA

Participants

AASEN David
California Institute of Technology, Pasadena, USA

ASMAR Mahmoud M.
Ohio University, Athens, USA

BAXEVANIS Benjamin
University of Hamburg, Germany

BEGUE Frédéric
IRSAMC, Toulouse, France

BELOPOLSKI Ilya
Princeton University, USA

COOK Ashley
University of Toronto, Canada

DASSONNEVILLE Bastien
Leibniz Institute IFW, Dresden, Germany

de COSTER George Joseph
University of Oregon, USA

FRUCHART Michel
ENS, Lyon, France

GANESH JAYA Sreejith
NORDITA, Stockholm, Sweden

GAZIT Snir
Israel Institute of Technology, Haifa, Israel

GERAEDTS Scott
California Institute, Pasadena, USA

GROMOV Andrey
Stony Brook University, USA

GRUSDT Fabian
University of Kaiserslautern, Germany

HALASZ Gabor
Rudolf Peierls Centre, Oxford, UK

HARPER Fenner
Rudolf Peierls Centre, Oxford, UK

HUANG Po-Hao
Boston University, USA

IADECOLA Thomas
Boston University, USA

JIAN Chaoming
Stanford University, USA

JONES Nicholas G.
University of Bristol, UK

KESELMAN Anna
Weizmann Institute, Rehovot, Israel

KOURTIS Stefanos
Leibniz Institute, Dresden, Germany

LIU Tianhan
UPMC, Ecole Polytechnique, Palaiseau, France

LUNDGREN Rex
University of Texas, Austin, USA

MORAMPUDI Siddhardh
Max Planck Institute, Dresden, Germany

MOTRUK Johannes
Max Planck Institute, Dresden, Germany

NAKOSAI Sho
University of Tokyo, Japan

NEUPERT Titus
Princeton University, USA

PENG Yang
Freie Universität Berlin, Germany

PETRESCU Tudor-Alexandru
Yale University, New Haven, USA and Ecole Polytechnique/CNRS Palaiseau, France

PETROVA Olga
Max Planck Institute, Dresden, Germany

PONTE Pedro
Perimeter Institute, Waterloo, Canada

POTASZ Pawel
Wroclaw University, Poland

QUEIROZ Raquel
Max Planck Institute, Stuttgart, Germany

QUELLE Anton
Utrecht University, Netherlands

QUITO Victor
University of Campinas, Brazil

RAOUX Arnaud
ENS Paris and Université Paris Sud, France

REHN Jorge Armando
Max Planck Institute, Dresden, Germany

RIEDER Maria-Theresa
University of Berlin, Germany

RISCHAU Willem
Ecole Polytechnique, Palaiseau, France

SANTOS Raul
Weizmann Institute, Rehovot, Israel

SBIERSKI Bjoern
University of Berlin, Germany

STICLET Doru Cristian
Université de Bordeaux, France

SÜSSTRUNK Roman
ETH, Zürich, Switzerland

TABERT Calvin
University of Guelph, Canada

TANG Evelyn
MIT, Cambridge, USA

TEKER Aykut
Sabanci University, Istanbul, Turkey

THAKURATHI Manisha
Indian Institute of Science, Bangalore, India

VAJNA Szabolcs
Budapest University, Hungary

VAYRYNEN Jukka
Yale University, New Haven, USA

WITCZACK-KREMPA William
Perimeter Institute, Waterloo, Canada

WU Yinghai
Pennsylvania University, University Park, USA

YOSHIMURA Yukinori
Hiroshima University, Japan

ZHANG Junyi
ENS, Paris, France

Part I

Basic Lectures

1

An introduction to topological phases of electrons

Joel E. Moore

University of California, Berkeley and
Lawrence Berkeley National Laboratory, USA

Topological Aspects of Condensed Matter Physics. First Edition. C. Chamon et al.

Chapter Contents

1.1 Introduction

These lectures seek to present a coherent picture of some key aspects of topological insulators and the quantum Hall effect. Rather than aiming for completeness or historical accuracy, the goal is to show that a few important ideas, such as the Berry phase and the Chern and Chern–Simons differential forms, occur repeatedly and serve as links between superficially different areas of physics. Non-interacting topological phases, electrical polarization, and some transport phenomena in metals can all be understood in a unified framework as consequences of Abelian and non-Abelian Berry phases. The fractional quantum Hall effect is then discussed as an example of topological order, and we introduce its description by the (Abelian) Chern–Simons topological field theory.

Some effort has been made to avoid duplicating the material covered in other Les Houches lectures, both past and present. Readers seeking alternative approaches and a comprehensive list of references are encouraged to consult the many review articles on topological insulators [16, 17, 35] and the recent book by Bernevig [4]. For the fractional quantum Hall effect, our treatment parallels closely the review article of Wen [40], and the Les Houches notes of Girvin [14] provide an overview of the topic that includes more physical background than we provide here.

As part of our goal is to explain the topological invariants that underlie various topological phases, we start in Section 1.2 with some preliminaries: a few examples of the two kinds of topology (homotopy and cohomology) that appear most frequently in condensed matter physics and a derivation of the Berry phase formula for adiabatic transport. No claims of rigour or completeness are made, and the book of Nakahara [30] is a good place to start learning more; readers focused on physics content should feel free to skip this section and refer back to it as necessary.

Section 1.3 introduces non-interacting topological phases of electrons (the integer quantum Hall effect and topological insulators are two important examples) and related phenomena, focusing on topological aspects. The concept of the Berry phase links these topological phases to important physical observables such as electrical polarization and the magnetoelectric effect.

Section 1.4 discusses topological phases in interacting systems, using a field-theory approach that starts with an example of topological terms in a conventional field theory (the Haldane gap in spin systems) and then moves on to the purely topological description of the fractional quantum Hall effect via Chern–Simons theory. Many additional steps in describing Chern–Simons field theory properly can be found in the Les Houches notes of Dunne [7]. While neither the interacting nor the non-interacting topological phases are discussed in full detail, it is hoped that this way of presenting them gives some practical understanding of what it means for an electronic state of matter to be 'topological'.

1.2 Basic concepts

1.2.1 Mathematical preliminaries

1.2.1.1 An intuitive example of global geometry and topology: Gauss–Bonnet

You may have heard a topologist described as 'a mathematician who can't tell the difference between a donut and a coffee cup'. As an example of the connections between

geometry and topology, we start by discussing an integral that will help us classify two-dimensional (2D) compact manifolds (surfaces without boundaries) embedded smoothly in three dimensions. The integral we construct is 'topologically invariant' in that if one such surface can be smoothly deformed into another, then the two will have the same value of the integral. The integral can't tell the difference between the surface of a coffee cup and that of a donut, but it can tell that the surface of a donut (a torus) is different from a sphere. Such global integrals of geometrical quantities are a common origin of topological quantities in physics.

We start with a bit of local geometry. Given our 2D surface in 3D, we can choose coordinates at any point on the surface so that the $(x, y, z = 0)$ plane is tangent to the surface, which can locally be specified by a single function $z(x, y)$. We choose $(x = 0, y = 0)$ to be the given point, so $z(0, 0) = 0$. The tangency condition is

$$\left.\frac{\partial z}{\partial x}\right|_{(0,0)} = \left.\frac{\partial z}{\partial y}\right|_{(0,0)} = 0. \tag{1.1}$$

Hence we can approximate z locally from its second derivatives:

$$z(x, y) \approx \frac{1}{2} \begin{pmatrix} x & y \end{pmatrix} \begin{pmatrix} \dfrac{\partial^2 z}{\partial x^2} & \dfrac{\partial^2 z}{\partial x\, \partial y} \\ \dfrac{\partial^2 z}{\partial y\, \partial x} & \dfrac{\partial^2 z}{\partial y^2} \end{pmatrix} \begin{pmatrix} x \\ y \end{pmatrix}. \tag{1.2}$$

The 'Hessian matrix' that appears here is real and symmetric. It can be diagonalized and has two real eigenvalues λ_1, λ_2, corresponding to two orthogonal eigendirections in the (x, y) plane. The geometric interpretation of these eigenvalues is simple: their magnitude is an inverse radius of curvature, and their sign tells us whether the surface is curving towards or away from the positive z direction in our coordinate system. To see why the first is true, suppose that we carried out the same process for a circle of radius r tangent to the x axis at the origin. Parametrize the circle by an angle θ that is 0 at the origin and traces the circle counterclockwise, i.e.

$$x = r \sin\theta, \qquad y = r(1 - \cos\theta). \tag{1.3}$$

Near the origin, we have

$$y = r\left[1 - \cos\left(\sin^{-1}\frac{x}{r}\right)\right] = r - \left(1 - \frac{x^2}{2r^2}\right) = \frac{x^2}{2r}, \tag{1.4}$$

which corresponds to an eigenvalue $\lambda = 1/r$ of the matrix in (1.2).

Going back to the Hessian, its determinant (the product of its eigenvalues, $\lambda_1\lambda_2$) is called the Gaussian curvature and has a remarkable geometric significance. First, consider a sphere of radius r, which at every point has $\lambda_1 = \lambda_2 = 1/r$. Then we can integrate the Gaussian curvature over the sphere's surface:

$$\int_{S^2} \lambda_1\lambda_2\, dA = \frac{4\pi r^2}{r^2} = 4\pi. \tag{1.5}$$

Beyond simply being independent of radius, this integral actually gives the same value for any compact manifold that can be smoothly deformed to a sphere.

However, we can easily find a compact manifold with a different value for the integral. Consider the torus made by revolving the circle in (1.3), with $r = 1$, around the axis of symmetry $x = t, y = -1, z = 0$, with $-\infty < t < \infty$. To compute the Gaussian curvature at each point, we sketch the calculation of the eigenvalues of the Hessian as follows. One eigenvalue is around the smaller circle, with radius of curvature r: $\lambda_1 = 1/r = 1$. Then the second eigenvalue must correspond to the perpendicular direction, which has a radius of curvature that depends on the angle θ around the smaller circle (we keep $\theta = 0$ to indicate the point closest to the axis of symmetry). The distance from the axis of symmetry is $2 - \cos\theta$, so we might have guessed $\lambda_2 = (2 - \cos\theta)^{-1}$, but there is an additional factor of $\cos\theta$ that appears because of the difference in direction between the surface normal and this curvature. So our guess is that

$$\lambda_2 = -\frac{\cos\theta}{2 - \cos\theta}. \tag{1.6}$$

As a check and to understand the sign, note that this predicts a radius of curvature 1 at the origin and other points closest to the symmetry axis, with a negative sign in the eigenvalue indicating that this curvature is in an opposite sense as that described by λ_1. At the top, the radius of curvature is 3 and in the same sense as that described by λ_1, and on the sides, λ_2 vanishes because the direction of curvature is orthogonal to the tangent vector.

Now we compute the curvature integral. With ϕ the angle around the symmetry axis, the curvature integral is

$$\begin{aligned} \int_{T^2} \lambda_1\lambda_2\, dA &= \int_0^{2\pi} d\theta \int_0^{2\pi} (2 - \cos\theta)\, d\phi\, \lambda_1\lambda_2 \\ &= \int_0^{2\pi} d\theta \int_0^{2\pi} d\phi\, (-\cos\theta) = 0. \end{aligned} \tag{1.7}$$

Again this zero answer is generic to any surface that can be smoothly deformed to the torus. The general result (the Gauss–Bonnet formula) of which the above are examples is

$$\int_S \lambda_1\lambda_2\, dA = 2\pi\chi = 2\pi(2 - g), \tag{1.8}$$

where χ is a topological invariant known as the Euler characteristic and g is the genus, essentially the number of 'holes' in the surface.[1] For a compact manifold with boundaries, the Euler characteristic becomes $2 - 2g - b$, where b is the number of

[1] A good question is why we write the Euler characteristic as $2 - 2g$ rather than $1 - g$; one way to motivate this is by considering polygonal approximations to the surface. The discrete Euler characteristic $V - E + F$, where V, E, and F count vertices, edges, and faces, respectively, is equal to χ. For example, the five Platonic solids all have $V - E + F = 2$.

boundaries: one can check this by noting that by cutting a torus, one can produce two discs (by slicing a bagel) or alternatively a cylinder with two boundaries (by slicing a Bundt cake).

More generally, we will encounter several examples where a topological invariant is expressed as an integral over a local quantity with a geometric significance. We now turn to a simpler example in order to allow us to introduce some basic concepts of algebraic topology.

1.2.1.2 Invariant integrals along paths in two dimensions: exact forms

As our first example of a topological property, let's ask about making line integrals along paths (not path integrals in the physics sense, where the path itself is integrated over[2]) that are nearly independent of the precise path: they will turn out to depend in some cases on topological properties (homotopy or cohomology). We will assume throughout these notes, unless otherwise specified, that all functions are smooth (i.e. $\mathbb{C}^\infty$, meaning derivatives of all orders exist).

First, suppose that we deal with paths on some open set U in the two-dimensional plane $\mathbb{R}^2$. (An open set is one for which some neighbourhood of each point in the set is also in the set.) We consider a smooth path $(u(t), v(t))$, where $0 \leq t \leq 1$ and the endpoints may be different[3]. Now let $f(x, y) = (p(x, y), q(x, y))$ be a two-dimensional vector field that lets us compute line integrals of this path:

$$W = \int_0^1 dt\, p\frac{du}{dt} + q\frac{dv}{dt}\, dt, \tag{1.9}$$

where p and q are evaluated at $(x(t), y(t))$.

Mathematical note In more fancy language, f is a differential form, a '1-form' to be precise. All that this means is that f is something we can use to form integrals over paths that are linear and probe the tangent vector of the path. Another way to state this, with which you may be more familiar, is that the tangent vector to a path, which we call a 'vector', transforms naturally in the opposite way to the gradient of a function, which we call a 'covector'. To convince yourself that this is true, think about how both transform under a linear transformation on the underlying space. We will say a bit more about such forms in a moment.

Our first goal is to show that the following three statements are equivalent:

(a) W depends only on the endpoints $(u(0), v(0))$ and $(u(1), v(1))$;
(b) $W = 0$ for any closed path;
(c) f is the gradient of a function g: $(p, q) = (\partial_x g, \partial_y g)$.

[2] There are additional topological properties that emerge ('quantum topology') when integrals over paths and other structures are incorporated; actually the Chern-Simons field theory that we discuss in Section 1.4 was an important tool in the history of that field.

[3] To make these results more precise, we should provide for adding one path to another by requiring only piecewise-smooth paths and require that u and v be smooth in an open set including $t \in [0, 1]$. For additional rigour, see the first few chapters of Fulton's book on algebraic topology [13].

The formal language used for (c) is that f is an *exact form*: $f = dg$ is the differential of a 0-form (a smooth function) g.

Note that (c) obviously implies (a) and (b), since then $W = g(u(1), v(1)) - g(u(0), v(0))$. To show that (b) implies (a), suppose (b) is true and (a) is not. Then there are two paths γ_1, γ_2 that have different integrals but the same endpoints. Form a new path γ so that, as t goes from 0 to $\frac{1}{2}$, γ_1 is traced, and then as t goes from $\frac{1}{2}$ to 1, γ_2 is traced opposite to its original direction (now you can see why piecewise-smooth paths are needed if one wants to be rigorous). Then this integral is non-zero, which contradicts (b).

It remains to show that (a) implies (c). Define $g(x, y)$ as equal to 0 at $(0, 0)$, or some other reference point in U if U does not include the origin. Everywhere else, set g equal to the W obtained by integrating over an arbitrary path from $(0, 0)$ to the final point, which by (a) is path-independent. (If U is not connected, then carry out this process on each connected component.) We will show that $\partial_x g = p$, and the same logic then implies $\partial_y g = q$. We need to compute

$$\partial_x g = \lim_{\Delta x \to 0} \frac{g(x + \Delta x, y) - g(x, y)}{\Delta x}. \tag{1.10}$$

We can obtain g by any path we like, so let's take an arbitrary path to define $g(x, y)$, then add a short horizontal segment to that path to define the path for $g(x + \Delta x, y)$. The value of the integral along this extra horizontal segment converges to $p(x, y)(\Delta x)$, as needed.

It turns out that the above case is simple because the plane we started with is 'topologically trivial'. Before proceeding to look at a non-trivial example, let us state one requirement on f that is satisfied whenever f is exact ($f = dg$). The fact that partial derivatives commute means that, with $f = dg = (p, q)$, $\partial_y p = \partial_x q$. We can come up with an elegant notation for this property by expanding our knowledge of differential forms.

Before, we obtained a 1-form f as the differential of a scalar g by defining

$$f = dg = \partial_x g \, dx + \partial_y g \, dy. \tag{1.11}$$

Note that we now include the differential elements dx, dy in the definition of f and that 1-forms form a real vector space (spanned by dx, dy): we can add them and multiply them by scalars. To obtain a 2-form as the differential of a 1-form, we repeat the process: writing $f = f_i \, dx_i$ (with $x_1 = x, x_2 = y, f_1 = p, f_2 = q$),

$$df = \sum_j \frac{\partial f_i}{\partial x_j} \, dx_j \wedge dx_i. \tag{1.12}$$

where the $\wedge$ product between differential forms satisfies the rule $dx_i \wedge dx_j = -dx_j \wedge dx_i$, which implies that if any coordinate appears twice, then we get zero: $dx \wedge dx = 0$. For some intuition about why this anticommutation property is important, note that in our 2D example,

$$df = (\partial_x f_y - \partial_y f_x) \, dx \wedge dy, \tag{1.13}$$

so that the function appearing in df is just the curl of the 2D vector field represented by f. So our statement about partial derivatives commuting is just the statement that if $f = dg$, then $df = 0$, or that the curl of a gradient is zero. We label any 1-form satisfying $df = 0$ a *closed form*. While every exact form is also closed, we will see that not every closed form is exact, with profound consequences.

1.2.1.3 Topologically invariant integrals along paths: closed forms

As an example of non-trivial topology, we would now like to come up with an example where integrals over paths are only path-independent in a limited 'topological' sense: the integral is the same for any two paths that are *homotopic*, one of the fundamental concepts of topology (to be defined in a moment). Basically, two paths are homotopic if one can be smoothly deformed into another. Consider the vector field

$$f = (p, q) = \left(-\frac{y}{x^2 + y^2}, \frac{x}{x^2 + y^2} \right) = \frac{-y\,dx + x\,dy}{x^2 + y^2}, \tag{1.14}$$

where in the second step we have used our 1-form notation. This vector field is well defined everywhere except the origin. This 1-form looks locally like the differential of $g = \tan^{-1}(y/x)$ (which just measures the angle in polar coordinates), but that function can only be defined smoothly on some open sets. For example, in a disc around the origin, the 2π ambiguity of the inverse tangent prevents us from defining g globally.

So, if we have a path that lies entirely in a region where g can be defined, then the integral of this 1-form over the path will give the change in angle between the starting point and end point, $g(u(1), v(1)) - g(u(0), v(0))$. What about other types of paths, for example, paths in $\mathbb{R}^2 \setminus (0, 0)$, the 2D plane with the origin omitted, that circle the origin and return to the starting point? We can still integrate using the 1-form f, even if it is not the gradient of a scalar function g, and will obtain the value $2\pi n$, where n is the 'winding number', a signed integer that describes how many times the closed path $(u(t), v(t))$ circles the origin as t goes from 0 to 1.

Now this winding number does not change as we make a small change in the closed path, as long as the path remains in $\mathbb{R}^2 \setminus (0, 0)$. What mathematical property of f guarantees this? We have seen that any exact 1-form (the differential of a scalar function) is also closed. While f is not exact, we can see that it is closed:

$$\begin{aligned} df &= \left(\partial_x \frac{x}{x^2 + y^2} \right) dx \wedge dy + \left(\partial_y \frac{-y}{x^2 + y^2} \right) dy \wedge dx \\ &= \frac{2 - 2}{x^2 + y^2} dx \wedge dy = 0. \end{aligned} \tag{1.15}$$

In other words, $(-y, x)/(x^2 + y^2)$ is curl-free ('irrotational'), while $(-y, x)$ has constant non-zero curl. Now suppose that we are given two paths γ_1 and γ_2 that differ by going in different ways around some small patch dA in which the 1-form remains defined. The difference in the integral of f over these two paths is then the integral of df over the enclosed surface by Stokes's theorem, which is zero if f is a closed form.

So we conclude that if f is a closed form, then the path integral is path-independent if we move the path through a region where f is always defined. For an exact form, the integral is completely path-independent. In the case of $\mathbb{R}^2 \setminus (0,0)$, the 1-form in (1.14) is locally but not completely path-independent. The set of closed forms and the set of exact forms are both vector spaces (we can add and multiply by scalars), which are typically infinite-dimensional, although their quotient as vector spaces is typically finite-dimensional. (The quotient of a vector space A by a vector space B is the vector space that identifies any two elements of A that differ only by an element of B.) A basic object in 'cohomology' is the first de Rham cohomology group (a vector space is by definition a group under addition):

$$H^1(M) = \frac{\text{closed 1-forms on } M}{\text{exact 1-forms on } M} = \frac{Z^1(M)}{B^1(M)}. \tag{1.16}$$

If you wonder why the prefix 'co-' appears in 'cohomology', there is a dual theory of linear combinations of curves, etc., called homology, in which the differential operator in de Rham cohomology is replaced by the boundary operator. However, while it may be equally more basic mathematically, homology seems to crop up less frequently in physics.

In this introductory discussion, we will focus on cohomology with real coefficients. The first and second Chern numbers defined later and applied to topological phases are related to elements of the even cohomology groups with *integer* coefficients $H^{2k}(M, \mathbb{Z})$. An even simpler object is the zeroth de Rham cohomology group. To understand this, realize that a closed 0-form is one whose gradient is zero, i.e. one that is constant on each connected component of U. There are no (-1)-forms and hence no exact 0-forms. So the zeroth group is just $\mathbb{R}^n$, where n is the number of connected components.

We can show that $H^1 = \mathbb{R}$ for the unit circle S^1 using the angle form f in (1.14), by showing that this form (more precisely, its equivalence class up to exact forms) provides a basis for H^1. Given some other form f', we use the unit-circle path, parametrized by an angle θ going from zero to 2π, to define

$$c = \frac{\int_0^{2\pi} f'}{\int_0^{2\pi} f}. \tag{1.17}$$

Now $f' - cf$ integrates to zero. We can define a function g via

$$g(\theta) = \int_0^{\theta} (f' - cf). \tag{1.18}$$

Now g is well defined and periodic because of how we defined c, and $f' = cf + dg$, which means that f' and cf are in the same equivalence class, because dg is an exact form. We say that f' and f are cohomologous because they differ by an exact form. So cf, $c \in \mathbb{R}$, generates H^1, and $H^1(S^1)$ is isomorphic to $\mathbb{R}$. With a little more work, one can show that $\mathbb{R}^2 \setminus (0,0)$ also has $H^1 = \mathbb{R}$.

Actually we can connect the results of this subsection to those of the previous one: a general expression for the Euler characteristic is

$$\chi(M) = \sum_i (-1)^i \dim H^i(M) = \sum_i (-1)^i \dim \frac{Z^i(M)}{B^i(M)}. \tag{1.19}$$

The dimension of the ith cohomology group is called the ith Betti number. To be pedantic, the Betti numbers are defined for homology rather than cohomology, but we can use a duality relationship. There is a compact way to express the idea of cohomology and homology that will let us introduce some notation and terminology. If Ω_r is the vector space of r-forms, and C_r is the dual space of r-chains, then the action of the boundary operator and the differential is as follows:

$$\longleftarrow C_r \underset{[\partial_{r+1}]}{\longleftarrow} C_{r+1} \underset{[\partial_{r+2}]}{\longleftarrow} C_{r+2} \longleftarrow, \tag{1.20}$$

$$\longrightarrow \Omega_r \underset{[d_{r+1}]}{\longrightarrow} \Omega_{r+1} \underset{[d_{r+2}]}{\longrightarrow} \Omega_{r+2} \longrightarrow. \tag{1.21}$$

The rth cohomology group is the quotient $\ker d_{r+1}/\mathrm{im}\, d_r$, and the rth homology group is $\ker \partial_r/\mathrm{im}\, \partial_{r+1}$.

The duality relationship is provided by Stokes's theorem. Recall that this theorem relates the integral of a form over a boundary to the integral of the differential of the form over the interior. In terms of the linear operator (f, c) that evaluates the form f on the chain c, we have the compact expression

$$(f, \partial c) = (df, c). \tag{1.22}$$

Now we move on to a different type of topology that is perhaps more intuitive and will be useful for our first physics challenge: how to classify defects in ordered systems.

1.2.1.4 Homotopy

What if we did not want to deal with smooth functions and calculus? An even more basic type of topology is homotopy theory, which can be defined without reference to calculus, differential forms, etc. Suppose that we are given a continuous map from $[0, 1]$ to a manifold M such that 0 and 1 get mapped to the same point; we can think of this as a closed curve on M. We say that two such curves γ_1, γ_2 are homotopic if there is a continuous function (a homotopy) f from $[0, 1] \times [0, 1]$ to M that satisfies

$$f(x, 0) = \gamma_1(x), \qquad f(x, 1) = \gamma_2(x). \tag{1.23}$$

Intuitively, f describes how to smoothly distort γ_1 to γ_2. Now, homotopy is an equivalence relation and hence defines equivalence classes: $[\gamma_1]$ is the set of all paths homotopic to γ_1. Furthermore, concatenation of paths (i.e. tracing one after the other) defines a natural group structure on these equivalence classes: the inverse of any path

can be obtained by tracing it in the opposite direction.[4] We conclude that the equivalence classes of closed paths form a group $\pi_1(M)$, called the fundamental group or first homotopy group. Higher homotopy groups $\pi_n(M)$ are obtained by considering mappings from the n-sphere S^n to M in the same way.

The homotopy groups of a manifold are not independent of the cohomology groups: for example, if $\pi_1(M)$ is trivial, then so is the first de Rham group. The cohomology groups are always Abelian; in general, the first de Rham group *with integer coefficients* is the Abelianization of π_1 (which need not be Abelian, although higher homotopy groups are). If you are interested in further details, the result of Hurewicz gives a relationship between higher cohomology and homotopy groups. The examples above of $\mathbb{R}^2 \setminus (0,0)$ and S^1 both have $\pi_1(M) = \mathbb{Z}$: there is an integer-valued winding number that we can use to classify paths, and this winding number can be computed by the angle form given above. So our 2D examples already contains the two types of topology that occur most frequently in physics: cohomology and homotopy. We will return to homotopy in much more detail in a moment, when we explain how it can be used to classify topological defects such as vortices in broken-symmetry phases.

1.2.1.5 Application of homotopy to topological defects in symmetry-breaking phases

As a direct physical application of homotopy theory, consider the notion of a 'vortex' in an ordered phase such as a superfluid. Such a configuration has a core where there is no order, but far away from the core the system is always locally in an ordered state. However, *which* ordered state the system is in varies smoothly as we move around the vortex core. For a 2D defect with a point core, such as a vortex of the 2D XY model, the vortex core is enclosed by a large real-space circle S^1, and as we move around this circle we have a map from S^1 to S^1, where the first circle is real space and the second circle reflects that the 'order-parameter manifold' of distinct ordered configurations of the XY model is also a circle.

The mathematical classification of topological defects has been carried out for a variety of systems. Vortex-like defects (defects that can be circled by a loop) are related to the group $\pi_1(M)$, where M is the manifold of degenerate values of the order parameter once its magnitude has been set (for example, S^1 for XY and S^2 for the Heisenberg model, where S^d is the unit sphere in $d+1$ dimensions). $\pi_1(M)$ is known as the first homotopy group and is the group of equivalence classes of mappings from S^1 to M: for example, the mappings from S^1 to S^1 are characterized by an integer winding number $n \in \mathbb{Z}$, so $\pi_1(S^1) = \mathbb{Z}$, while $\pi_1(S^2) = 0$ (the group with one element), since any loop on the sphere is contractible to a point.

In other words, $\pi_1(M)$ gives the set of equivalence classes up to smooth deformations of closed paths on M. Multiplication of equivalence classes in the group is defined by concatenation of paths. The second homotopy group $\pi_2(M)$ classifies mappings from S^2 to M, and describes defects circled by a sphere, such as pointlike defects

[4] To be precise, one should define homotopy with reference to a particular point where paths start and end; for a symmetric space where all points are basically equivalent, this is unnecessary.

in 3D. For example, $\pi_2(S^2)$ is non-zero, and there are stable point defect configurations of Heisenberg spins (known descriptively as 'hedgehogs') but not of XY spins. There can also be topological configurations that are not 'defects' but are not homotopic to the identity: the most famous example is the skyrmion configuration of a uniaxial ferromagnet in 2D, where all spins at infinity point in the same direction and the spin direction moves in the plane in such a way as to cover the sphere once. Shankar's monopoles and other defect-free configurations in 3D are related to the group π_3.

There is a considerable technology built up for the calculation of homotopy groups of general order-parameter manifolds $M = G/H$, whose elements are cosets of the residual symmetry group H, i.e. any symmetries that survive in the ordered phase, in the high-temperature symmetry group G. For example, for a uniaxially ordered Heisenberg ferromagnet, $G = SO(2)$ and $H = SO(3)$, so indeed $M = S^2$ as anticipated earlier. The advent of complicated ordered states in systems such as liquid crystals and spinor condensates stimulated the development of the techniques described in the *Review of Modern Physics* article by Mermin [25].

1.2.2 Berry phases in quantum mechanics

We now turn to a beautiful geometric property of quantum mechanics that was understood relatively recently: the geometric or Berry phase. The connection to the Gauss–Bonnet theorem we mentioned earlier is as follows. Curvature is a property of Riemannian manifolds, which have a (real) inner product defined on the tangent space at each point.[5] This inner product varies smoothly from point to point, which allows us to define a number of important concepts, including parallel transport and curvature.

Frequently in quantum mechanics, we have, instead of a tangent space, a Hilbert space (including a Hermitian inner product) that varies smoothly from point to point in parameter space. Hence one can think of the Berry-phase objects we are about to define as really quite similar to curvature and related properties on Riemannian manifolds, except that the Berry phase does not come from the intrinsic geometry of the manifold of parameters but rather is related to how the attached Hilbert space evolves as parameters change.

An important result from undergraduate quantum mechanics is the 'adiabatic approximation'. Suppose that a system is prepared in a non-degenerate eigenstate of a time-dependent Hamiltonian H. For later reference, we will write H as a function of some parameters λ_i that depend on time: $H(t) = H(\lambda_1(t), \lambda_2(t), \ldots)$. If the eigenstate remains non-degenerate, then the adiabatic approximation is the result that if the Hamiltonian changes slowly in time (how slowly depends primarily on the energy gap between adjacent eigenstates), then there are no transitions between eigenstates.

This approximation, even when correct, only gives part of the story: it describes the probability to remain in the eigenstate that evolved from the initial eigenstate, but

[5] The combination of a differentiable manifold and its tangent space at each point is the 'tangent bundle', the simplest example of a vector bundle, an attachment of a vector space to each point of a manifold.

there is actually non-trivial information in the *phase* of the final state as well. This result may seem quite surprising because the overall phase in quantum mechanics is in general independent of observable quantities. However, the Berry phase from an adiabatic evolution is observable: for example, one system can be taken around a closed path in parameter space, while another system initially identical to the first can be taken around a different path, or the null path; an interference experiment on the final states will reveal the Berry phase. The first example of this type of geometric phase in physics was found more than 50 years ago by Pancharatnam in an optical example, but Berry's classic paper of 1984 was the first to explain the concept in its full generality.

Berry's result for a closed path is relatively simple to state, but some careful thought is required to understand and derive it. In moving a system adiabatically around a closed path in parameter space, the final wavefunction is in the same eigenstate as the initial one (again, under the assumptions of the adiabatic approximation as stated above), but its phase has changed:

$$|\psi(t_f)\rangle = \exp\left[-\frac{i}{\hbar}\oint_{t_i}^{t_f} E(t')\,dt'\right] e^{i\gamma}|\psi(t_i)\rangle. \tag{1.24}$$

Here $E(t')$ means the corresponding eigenvalue of the Hamiltonian at that time, and γ is the Berry phase, expressed as an integral over a path in *parameter* space with no time dependence:

$$\gamma = i\int \langle\tilde{\psi}(\lambda_i)|\nabla_{\boldsymbol{\lambda}}|\tilde{\psi}(\lambda_i)\rangle \cdot d\boldsymbol{\lambda}. \tag{1.25}$$

Note that there are two different wavefunctions ψ and $\tilde{\psi}$ in the above formulas. $\psi(t)$ has a time argument and means the wavefunction of the system at that time. The 'reference wavefunction' $\tilde{\psi}(\lambda_i)$ has a parameter argument and indicates the wavefunction we have chosen of the Hamiltonian for that value of the parameters, which we assume to be smoothly varying[6] A key assumption of the following derivation is that there is some smooth choice of the $\tilde{\psi}(\lambda_i)$ throughout a surface in parameter space with the loop as boundary.

For an open path, we need to describe the phase of the wavefunction relative to this reference set, so the expression becomes more complicated (for the closed path, we could simply compare the initial and final wavefunctions, without needing the reference set at these points). We will show that, assuming $\psi(t_i) = \tilde{\psi}(\lambda(t_i))$ so that

[6] A smooth choice of reference wavefunctions is always possible locally but not possible globally, as in the example of a spin-$\frac{1}{2}$ particle moving in a Zeeman magnetic field. Computing the Berry phase in this example is a nice exercise for the reader, and also physically useful: in making a path integral for a quantum spin, one needs to include a term that reflects the Berry phase of the path in time (either real or imaginary), and we will use this in Section 1.4. A pedagogical derivation of this path integral including the Berry phase is in the book of Auerbach [2].

the initial wavefunction is equal to the reference state at the corresponding value of parameters,

$$\langle\tilde{\psi}(\lambda_i(t))|\psi(t)\rangle = \exp\left[-\frac{i}{\hbar}\int_0^t E(t')\,dt'\right]e^{i\gamma} \equiv e^{i\theta(t)}, \tag{1.26}$$

i.e. the Berry phase appears as an extra contribution, beyond the expected contribution related to the energy, when comparing the actual time-dependent evolved state $\psi(t)$ with the reference state at the same point in parameter space $\lambda_i(t)$. We write $\theta(t)$ for the total phase including both energetic and Berry contributions. We can take the time derivative using the time-dependent Schrödinger equation

$$i\hbar\frac{\partial\psi}{\partial t} = H(t)\psi. \tag{1.27}$$

The first two quantities in (1.26) agree initially from our choice of the phase of $\psi(t_i)$. The time derivative of the leftmost is

$$\langle\tilde{\psi}(\lambda_i(t))|\,\frac{-iE(t)}{\hbar}\,|\psi(t)\rangle + \frac{d\lambda_j}{dt}\langle\partial_{\lambda_j}\tilde{\psi}(\lambda_i(t))|\psi(t)\rangle, \tag{1.28}$$

Since $e^{i\theta(t)} = \langle\psi(\lambda_i(t))|\psi(t)\rangle$, this gives

$$\begin{aligned} i\partial_t\theta(t) &= i\left(\frac{d}{dt}e^{i\theta(t)}\right)(-ie^{-i\theta(t)}) \\ &= \left[\frac{-iE(t)}{\hbar}\langle\tilde{\psi}(\lambda_i(t))| + \frac{d\lambda_j}{dt}\langle\partial_{\lambda_j}|\tilde{\psi}(\lambda_i(t))|\right]|\psi(t)\rangle\langle\psi(t)|\tilde{\psi}(\lambda_i(t))\rangle, \end{aligned} \tag{1.29}$$

and this is satisfied if we set (note that for E we do not need to distinguish between time and λ dependence)

$$\partial_t\theta(t) = -\frac{E(t)}{\hbar} - i\frac{d\lambda_j}{dt}\langle\partial_{\lambda_j}\tilde{\psi}(\lambda_i(t))|\tilde{\psi}(\lambda_i(t))\rangle, \tag{1.30}$$

which is our desired conclusion. We have used the fact that ψ and $\tilde{\psi}$ differ only by a phase factor, since they describe the same non-degenerate state, to eliminate $|\psi\rangle\langle\psi|$.

The 'Berry connection' or 'Berry vector potential' $A_j = i\langle\psi(\lambda_i)|\partial_{\lambda_j}\psi(\lambda_i)\rangle$ is real, which follows from noting that $\partial_{\lambda_j}\langle\tilde{\psi}((\lambda_i)|\tilde{\psi}(\lambda_i)\rangle = 0$ by constancy of normalization. It is required for a non-zero Berry phase that H evolve in such a way that the wavefunction changes by more than just a phase, so that that the evolution of the wavefunction is more than just a simple phase factor, even though the actual rate of change in H drops out and only the path taken by H enters the Berry phase.

Now one can ask whether the Berry connection $\mathbf{A}$ is independent of how we chose the reference wavefunctions (in this case, the $U(1)$ degree of freedom in the wavefunction at each λ). While for an open path the Berry phase is clearly not phase-independent, it is so for a closed path—for exactly the same reasons as a closed line integral of $\mathbf{A}$ is gauge-independent in electrodynamics: we can integrate the 'Berry

flux' or 'Berry curvature' $\epsilon_{ij}\partial_i A_j$ (which you can check is phase-independent, just like $F_{\mu\nu}$ in electrodynamics) on the surface bounded by the path. Alternatively, we can note that a phase change changes A by the gradient of a scalar, so that on a closed loop there is no change.

Independent of Berry's work and at roughly the same time, condensed matter physicists such as Thouless were realizing that Berry phases of wavefunctions on the Brillouin zone have the same mathematical structure as gauge fields in parameter space, even though there is no longer a notion of time evolution. The Berry vector potential $\mathbf{A}$ is a way to compare or 'connect' the Hilbert spaces at neighbouring points in parameter space. The gauge-invariant or nearly gauge-invariant quantities constructed from $\mathbf{A}$ and its derivatives control a variety of physical quantities. For the specific case of wavefunctions on the Brillouin zone, we will see that $\mathbf{A}$ is intimately related to the location of the wavefunctions within the unit cell in real space.

To get some geometric intuition for what the Berry phase means in general, we explain why the Berry connection A is called a connection, and the flux F is sometimes called a curvature. A connection is a way to compare vector spaces that are attached to different points of a manifold, forming a 'vector bundle'. In our case, there is a one-dimensional complex vector space attached at each point in parameter space, spanned by the local eigenstate. The inner product lets us compare vectors at the same point in parameter space, but the Berry connection appears when we try to compare two vectors from slightly different points.

An example we used above of a real vector bundle is the 'tangent bundle' to a Riemannian manifold (say, a sphere), made up of tangent vectors at each point, which have a dot product corresponding to the inner product in quantum mechanics. The connection in this case, which gives rise to 'parallel transport' of tangent vectors, is related to the same curvature that we previously discussed with the Gauss–Bonnet theorem. Consider an aeroplane moving around the surface of the Earth and carrying a gyroscope that is fixed to lie in the tangent plane to the Earth's surface (i.e. free to rotate around the normal axis to the tangent plane). If the aeroplane follows a great circle, then it will appear to be going straight ahead to a passenger on board, and the gyroscope will not rotate relative to the plane's axis.

However, if the aeroplane follows a line of latitude other than the equator, or any other path that is not a 'geodesic' (see a differential geometry text for details), it will feel constantly as though it is turning, and the gyroscope will appear to rotate relative to the aeroplane's direction. After going around a closed path in the aeroplane, the gyroscope may have rotated compared with a stationary gyroscope (the same physics that underlies Foucault's pendulum). As an exercise, you can work out that the total angle of rotation in circling a line of latitude is $2\pi \sin(\phi)$, where ϕ is the latitude. At the equator this gives no rotation, while at the north pole it gives a 2π rotation. This is a geometrical version of the same idea of holonomy (failure of a gyroscope to return to its initial direction) that underlies the Berry phase.

Note that a vector potential in a gauge theory and the associated Wilson loop are also examples of the concept of holonomy in a (now complex) vector bundle. The $U(1)$ Berry phase described above generalizes immediately to a non-Abelian $U(N)$ Berry phase when there are degenerate states or the energy differences between states are

irrelevant, which has some important applications in condensed matter physics that have only recently been discovered. Our primary mathematical objects later in this chapter will be properties of the wavefunctions on the Brillouin zone, which form a Hermitian bundle (a smoothly varying Hilbert space) on the d-dimensional torus.

One reason for introducing the idea of cohomology above was to give a sense of the mathematical structures hiding in the background of the simple calculations we do: to pick one example, the integral physicists do to calculate the Chern number, which determines the contribution of a filled 2D band to the quantum Hall effect, would be viewed by a mathematician as using the first Chern form to classify smooth complex line bundles on the Brillouin zone, and the group of line bundles under tensor products is isomorphic to the second cohomology class with integer coefficients. However, our hope is that the physical examples we discuss will be readily comprehensible even for readers not terribly excited about algebraic technology.

1.3 Topological phases: Thouless phases arising from Berry phases

The integer quantum Hall effect (IQHE) has the remarkable property that, even at finite temperature in a disordered material, a transport quantity is quantized to remarkable precision: the transverse (a.k.a. Hall) conductivity is $\sigma_{xy} = ne^2/h$, where n is integral to 1 part in 10^9. This quantization results because the transport is determined by a topological invariant, as stated most clearly in the work of Thouless and collaborators. Consequently, we use the term 'Thouless phases' for phases where a response function is determined by a topological invariant.

In the cases we discuss, including the recently discovered 'topological insulators' and quantum spin Hall effect (QSHE), this topological invariant results from integration of an underlying Berry phase. It turns out that the Berry phase can be rather important even when it is not part of a topological invariant. In crystalline solids, the electrical polarization, the anomalous Hall effect, and the magnetoelectric polarizability all derive from Berry phases of the Bloch electron states, which are introduced in the following subsection. We will avoid the conventional textbook presentation of the IQHE in terms of Landau levels of a continuum electron. As we will use Landau levels when we discuss the fractional quantum Hall effect later, readers who are unfamiliar with the IQHE may wish to learn the standard treatment (see e.g. [14]) and compare it with the approach using Bloch electrons below. The connection between the two can be made precise in the limit of small flux per unit cell, when a flat magnetic Bloch band becomes equivalent to a Landau level.

1.3.1 Bloch states

One of the cornerstones of the theory of crystalline solids is Bloch's theorem for electrons in a periodic potential. We will demonstrate this in the following form: given a potential invariant under a set of lattice vectors $\mathbf{R}$, $V(\mathbf{r}+\mathbf{R}) = V(\mathbf{r})$, the electronic eigenstates can be labelled by a 'crystal momentum' $\mathbf{k}$ and written in the form

$$\psi_{\mathbf{k}}(\mathbf{r}) = e^{i\mathbf{k}\cdot\mathbf{r}} u_{\mathbf{k}}(\mathbf{r}), \tag{1.31}$$

where the function u has the periodicity of the lattice. Note that the crystal momentum $\mathbf{k}$ is only defined up to addition of reciprocal lattice vectors, i.e. vectors whose dot product with any of the original lattice vectors is a multiple of 2π.

We give a quick proof of Bloch's theorem in one spatial dimension, then consider the Berry phase of the resulting wavefunctions. A standard fact from quantum mechanics tells us that, given two Hermitian operators that commute, we can find a basis of simultaneous wavefunctions. In the problem at hand, we have a non-Hermitian operator (lattice translations by the lattice spacing a: $(T\psi)(x) = \psi(x+a)$) that commutes with the Hamiltonian. It turns out that only one of the two operators needs to be Hermitian for simultaneous eigenstates to exist, and therefore we can find wavefunctions that are energy eigenstates and satisfy

$$(T\psi)(x) = \lambda\psi(x). \tag{1.32}$$

Now if the magnitude of λ is not 1, repeated application of this formula will give a wavefunction that either blows up at spatial positive infinity or negative infinity. We would like to find wavefunctions that can extend throughout an infinite solid with bounded probability density, and hence require $|\lambda| = 1$. From this, it follows that $\lambda = e^{i\theta}$, and we define $k = \theta/a$, where we need to specify an interval of width 2π to uniquely define θ, say $[-\pi, \pi)$. In other words, k is ambiguous by addition of a multiple of $2\pi/a$, as expected. So we have shown

$$\psi_k(x+a) = e^{ika}\psi_k(x). \tag{1.33}$$

The last step is to define $u_k(x) = \psi_k(x)e^{-ikx}$; then (1.33) shows that u_k is periodic with period a, and $\psi_k(x) = e^{ikx}u_k(x)$. [7]

While the energetics of Bloch wavefunctions underlies many properties of solids, there is also Berry-phase physics arising from the dependence of u_k on k that was understood only rather recently. Note that, even though this is one-dimensional, there is a non-trivial 'closed loop' in the parameter k that can be defined because of the periodicity of the 'Brillouin zone' $k \in [-\pi/a, \pi/a)$:

$$\gamma = \oint_{-\pi/a}^{\pi/a} \langle u_k | i\partial_k | u_k \rangle \, dk. \tag{1.34}$$

How are we to interpret this Berry phase physically, and is it even gauge-invariant? We will derive it from scratch below, but an intuitive clue is provided if we make the replacement $i\partial_k$ by x, as would be appropriate if we consider the action on a plane wave. This suggests, correctly, that the Berry phase may have something to do with the spatial location of the electrons, but evaluating the position operator in a Bloch state gives an ill-defined answer; for this real-space approach to work, we would need to introduce localized 'Wannier orbitals' in place of the extended Bloch states.

[7] Readers interested in more information and the 3D case can consult any solid state physics text, e.g. Ashcroft and Mermin [1].

Another clue to what the phase γ might mean physically is provided by asking if it is gauge-invariant. Before, gauge-invariance resulted from assuming that the wavefunction could be continuously defined on the interior of the closed path. Here we have a closed path on a noncontractible manifold; the path in the integral winds around the Brillouin zone, which has the topology of the circle. What happens to the Berry phase if we introduce a phase change $\phi(k)$ in the wavefunctions, $|u_k\rangle \to e^{-i\phi(k)}|u_k\rangle$, with $\phi(\pi/a) = \phi(-\pi/a) + 2\pi n, n \in \mathbb{Z}$? Under this transformation, the integral shifts as

$$\gamma \to \gamma + \oint_{-\pi/a}^{\pi/a} (\partial_k \phi)\, dk = \gamma + 2\pi n. \tag{1.35}$$

So, redefinition of the wavefunctions shifts the Berry phase. This corresponds to changing the polarization by a multiple of the 'polarization quantum', which in one dimension is just the electron charge. (In higher dimensions, the polarization quantum is one electron charge per transverse unit-cell area.) Physically, the ambiguity of polarization corresponds to the following idea: given a system with a certain bulk unit cell, there is an ambiguity in how that system is terminated and how much surface charge is at the boundary; adding an integer number of charges to one allowed termination gives another allowed termination [37]. The Berry phase is not gauge-invariant, but any fractional part it had in units of a *is* gauge-invariant. However, the above calculation suggests that, to obtain a gauge-invariant quantity, we need to consider a two-dimensional crystal rather than a one-dimensional one. Then integrating the Berry curvature, rather than the Berry connection, has to give a well-defined gauge-invariant quantity.

We will give a physical interpretation of γ in the next section as a 1D polarization by relating changes in γ to electrical currents. (A generalization of this Berry phase is remarkably useful for the theory of polarization in real, 3D materials.) In the next section, we will understand how this 1D example is related to the 2D IQHE. Historically, the understanding of Berry phases in the latter came first, in a paper by Thouless, Kohmoto, den Nijs, and Nightingale [39]. They found that when a lattice is put in a commensurate magnetic field (one with rational flux per unit cell, in units of the flux quantum so that Bloch's theorem applies), each occupied band j contributes an integer

$$n_j = \frac{i}{2\pi} \int dk_x\, dk_y \, \left(\langle \partial_{k_x} u_j | \partial_{k_y} u_j \rangle - \langle \partial_{k_y} u_j | \partial_{k_x} u_j \rangle \right) \tag{1.36}$$

to the total Hall conductance:

$$\sigma_{xy} = \frac{e^2}{h} \sum_j n_j. \tag{1.37}$$

Now we derive this topological quantity (the 'Chern number', expressed as an integral over the Berry flux, which is the curl of the Berry connection $A^j = i\langle u_j | \nabla_k u_j \rangle$) for the case of 1D polarization, then explain its mathematical significance.

1.3.2 1D polarization and 2D IQHE

We start with the question of 1D polarization mentioned earlier. More precisely, we attempt to compute the change in polarization by computing the integral of current through a bulk unit cell under an adiabatic change:

$$\Delta P = \int_0^1 d\lambda \, \frac{dP}{d\lambda} = \int_{t_0}^{t_1} dt \, \frac{dP}{d\lambda}\frac{d\lambda}{dt} = \int_{t_0}^{t_1} j(t)\, dt. \tag{1.38}$$

In writing this formula, we are assuming implicitly that there will be some definition of dP in terms of a parameter λ of the bulk Hamiltonian. Our treatment will follow that of Resta [37], but with a few more mathematical details in the derivation. (We write q for 1D momentum and k_x, k_y for 2D momenta in the following.) We will use Bloch's theorem in the following form: the periodic single-particle orbitals $u_n(q, r)$ are eigenstates of

$$H(q, \lambda) = \frac{1}{2m}(p + \hbar q)^2 + V^{(\lambda)}(r). \tag{1.39}$$

The current operator is

$$j(q) = ev(q) = \frac{ie}{\hbar}[H(q, \lambda), r] = \frac{e}{m}(p + \hbar q) = \frac{e}{\hbar}\partial_q H(q, \lambda). \tag{1.40}$$

The current at any fixed λ in the ground state is zero, but changing λ adiabatically in time drives a current that generates the change in polarization. To compute this current, we need to use the first correction to the adiabatic theorem (cf. the quantum mechanics book of Messiah [26]). Following Thouless, we choose locally a gauge in which the Berry phase is zero (this can only be done locally and is only meaningful if we obtain a gauge-invariant answer for the instantaneous current) and write for the many-body wavefunction

$$|\psi(t)\rangle = \exp\left[-\frac{i}{\hbar}\int^t E_0(t')\, dt'\right]\left[|\psi_0(t)\rangle + i\hbar \sum_{j\neq 0} |\psi_j(t)\rangle (E_j - E_0)^{-1} \langle \psi_j(t)|\dot{\psi}_0(t)\rangle\right]. \tag{1.41}$$

Here $E_i(t)$ are the local eigenvalues and $|\psi_j(t)\rangle$ a local basis of reference states. The first term is just the adiabatic expression we derived before, but with the Berry phase eliminated with a phase rotation to ensure $\langle\psi_0(t)|\dot{\psi}_0(t)\rangle = 0$.

We want to use the above expression to write the expectation value of the current. The ground state must differ from the excited state by a single action of the (one-body) current operator, which promotes one valence electron (i.e. an electron in an occupied state) to a conduction electron. Using the one-particle states, we get

$$\frac{dP}{d\lambda} = 2\hbar e \,\mathrm{Im} \sum_{v,c} \int \frac{dq}{2\pi} \frac{\langle u_v(q)|v(q)|u_c(q)\rangle\langle u_c(q)|\partial_\lambda u_v(q)\rangle}{E_c(q) - E_v(q)}. \tag{1.42}$$

For example, we wrote

$$\langle \psi_j(t)|\dot{\psi}_0(t)\rangle = \sum_{v,c}\langle u_c|\partial_\lambda u_v\rangle \frac{d\lambda}{dt}. \tag{1.43}$$

This sum involves both valence and conduction states. For simplicity, we assume a single valence state in the following. We can rewrite the sum simply in terms of the valence state using the first-order time-independent perturbation theory expression for the wavefunction change under a perturbation Hamiltonian $H' = dq\,\partial_q H$:

$$|\partial_q u_j(q)\rangle = \sum_{j\neq j'} |u_{j'}(q)\rangle \frac{\langle u_{j'}(q)|\partial_q H(q,\lambda)|u_j(q)\rangle}{E_j(q) - E_{j'}(q)}. \tag{1.44}$$

Using this and $v(q) = \hbar^{-1}\partial_q H(q,\lambda)$, we obtain

$$\begin{aligned}\frac{dP}{d\lambda} &= 2\hbar e\,\mathrm{Im}\sum_c \int \frac{dq}{2\pi}\frac{\langle u_v(q)|v(q)|u_c(q)\rangle\langle u_c(q)|\partial_\lambda u_v(q)\rangle}{E_c(q) - E_v(q)} \\ &= 2e\,\mathrm{Im}\int \frac{dq}{2\pi}\langle \partial_q u_v(q)|\partial_\lambda u_v(q)\rangle.\end{aligned} \tag{1.45}$$

We can convert this to a change in polarization under a finite change in parameter λ:

$$\Delta P = 2e\,\mathrm{Im}\int_0^1 d\lambda \int \frac{dq}{2\pi}\langle \partial_q u_v(q)|\partial_\lambda u_v(q)\rangle. \tag{1.46}$$

The last expression is in 2D and involves the same type of integrand (a Berry flux) as in the 2D TKNN formula (1.36). However, in the polarization case, there does not need to be any periodicity in the parameter λ. If this parameter is periodic, so that $\lambda = 0$ and $\lambda = 1$ describe the same system, then the total current run in a closed cycle that returns to the original Hamiltonian must be an integer number of charges, consistent with quantization of the TKNN integer in the IQHE.

If we define polarization via the Berry connection,

$$P = ie \int \frac{dq}{2\pi}\langle u_v(q)|\partial_q u_v(q)\rangle, \tag{1.47}$$

so that its derivative with respect to λ will give the result above with the Berry flux, we note that a change of gauge changes P by an integer multiple of the charge e. Only the fractional part of P is gauge-independent. Note that u and the Bloch Hamiltonian are not generally periodic with the Brillouin zone, even though the energy levels and Berry curvature are. This does not affect the calculation of topological invariants, but it does matter for evaluating the polarization via (1.47). The relationship between polarization in 1D, which has an integer ambiguity, and the IQHE in 2D, which has an integer quantization, is the simplest example of the relationship between Chern–Simons forms in odd dimension and Chern forms in even dimension. We will turn soon to the mathematical properties of these differential forms, which in the case above (and others to be discussed) came from the Berry phases of a band structure.

1.3.3 Interactions and disorder: the flux trick

One might worry whether the TKNN integer defined in (1.36) is specific to non-interacting electrons in perfect crystals. An elegant way to generalize the definition physically, while keeping the same mathematical structure, was developed by Niu, Thouless, and Wu [31]. This definition also makes somewhat clearer, together with our polarization calculation above, why this invariant should describe σ_{xy}. First, note that from the formula for the Bloch Hamiltonian in the polarization calculation above, we can reinterpret the crystal momentum q as a parameter describing a flux threaded through a unit cell of size a: the boundary conditions are periodic up to a phase $e^{iqa} = e^{ie\Phi/\hbar c}$. We will start by reinterpreting the non-interacting case in terms of such fluxes, then move to the interacting case.

The setup is loosely similar to the Laughlin argument for quantization in the IQHE. Consider adiabatically pumping a flux Φ_x though one circle of a toroidal system, in the direction associated with the periodicity $x \to x + L_x, y \to y$. The change in this flux in time generates an electric field pointing in the $\hat{\mathbf{x}}$ direction. Treating this flux as a parameter of the crystal Hamiltonian, we compute the resulting change in $\hat{\mathbf{y}}$ polarization, which is related to the y current density:

$$\frac{dP_y}{dt} = j_y = \frac{dP_y}{d\Phi_x}\frac{d\Phi_x}{dt} = \frac{dP_y}{d\Phi_x}(cE_xL_x). \tag{1.48}$$

We are going to treat the polarization P_y as an integral over y flux but keep Φ_x as a parameter. Then [32]

$$P_y(\Phi_x) = \frac{ie}{2\pi}\int d\Phi_y \langle u|\partial_{\Phi_y} u\rangle \tag{1.49}$$

and we see that polarization now has units of charge per length, as expected. In particular, the polarization quantum in the y direction is now one electronic charge per L_x. The last step to obtain the quantization is to assume that we are justified in averaging j_y over the flux:

$$\langle j_y\rangle = \left\langle \frac{dP_y}{d\Phi_x}\right\rangle (cE_xL_x) \to \frac{\Delta P_y}{\Delta\Phi_x}(cE_xL_x), \tag{1.50}$$

where Δ means the change over a single flux quantum, $\Delta\Phi_x = hc/e$. So the averaged current is determined by how many y-polarization quanta change in the periodic adiabatic process of increasing the x flux by hc/e:

$$\langle j_y\rangle = \frac{e}{hc}\frac{ne}{L_x}(cE_xL_x) = \frac{ne^2}{h}E_x. \tag{1.51}$$

The integer n follows from noting that computing $dP_y/d\Phi_x$ and then integrating $d\Phi_x$ gives just the expression for the TKNN integer (1.36), now in terms of fluxes.

1.3.4 TKNN integers, Chern numbers, and homotopy

In this subsection, we will give several different ways to understand the TKNN integer or Chern number described above. First, a useful trick for many purposes is to define the Berry flux and first Chern number in a manifestly gauge-invariant way, using projection operators. For the case of a single non-degenerate band, define $P_j = |u_j\rangle\langle u_j|$ at each point of the Brillouin zone. This projection operator is clearly invariant under $U(1)$ transformations of u_j. The Chern number can be obtained as

$$n_j = \frac{i}{2\pi} \int \mathrm{Tr}\left[dP_j \wedge P_j \, dP_j\right], \tag{1.52}$$

where $\wedge$ is the wedge product and $dP_j = \partial_{k_x} P_j \, dk_x + \partial_{k_y} P_j \, dk_y$ is a differential form where the coefficients are operators. (Note that the wedge product in the above formula acts only on dk_x and dk_y.) It is a straightforward exercise to verify that this reproduces the TKNN definition (1.36).

Then the generalization to degenerate bands, for example, is naturally studied by using the gauge- and basis-invariant projection operator $P_{ij} = |u_i\rangle\langle u_i| + |u_j\rangle\langle u_j|$ onto the subspace spanned by $|u_i\rangle$ and $|u_j\rangle$: the index of this operator gives the total Chern number of bands i and j. In general, when two bands come together, only their total Chern number is defined. The total Chern number of all bands in a finite-dimensional band structure (i.e. a finite number of bands) is argued to be zero below. Often one is interested in the total Chern number of all occupied bands because this describes the IQHE through the TKNN formula; because of this zero-sum rule, the total Chern number of all *unoccupied* bands must be equal and opposite.

In the remainder of this subsection, we use a powerful homotopy argument of Avron, Seiler, and Simon to show indirectly that there is one Chern number per band, but with a 'zero-sum rule' that all the Chern numbers add up to zero. We will not calculate the Chern number directly, but rather the homotopy groups of Bloch Hamiltonians. To get some intuition for the result, we first consider the example of a non-degenerate two-band band structure, then give the general result, which is an application of the 'exact sequence of a fibration'.

The Bloch Hamiltonian for a two-band non-degenerate band structure can be written in terms of the Pauli matrices and the two-by-two identity as

$$H(k_x, k_y) = a_0(k_x, k_y)\mathbf{1} + a_1(k_x, k_y)\sigma_x + a_2(k_x, k_y)\sigma_y + a_3(k_x, k_y)\sigma_z. \tag{1.53}$$

The non-degeneracy constraint is that a_1, a_2, and a_3 are not all simultaneously zero. Now we first argue that a_0 is only a shift in the energy levels and has no topological significance, i.e. it can be smoothly taken to zero without a phase transition. Similarly, we can deform the other a functions to describe a unit vector on $\mathbb{Z}_2$: just as the punctured plane $\mathbb{R}^2 \setminus (0,0)$ can be taken to the circle, we are taking punctured 3-space to the 2-sphere via

$$(a_1, a_2, a_3) \to \frac{(a_1, a_2, a_3)}{\sqrt{{a_1}^2 + {a_2}^2 + {a_3}^2}} \tag{1.54}$$

at each point in k-space.

Now we have a map from T^2 to S^2. We need to use one somewhat deep fact: under some assumptions, if $\pi_1(M) = 0$ for some target space M, then maps from the torus $T^2 \to M$ are contractible to maps from the sphere $S^2 \to M$. Intuitively, this is because the images of the non-contractible circles of the torus, which make it different from the sphere, can be contracted on M. By this logic, the two-band non-degenerate band structure in 2D is characterized by a single integer, which can be viewed as the Chern number of the occupied band.

What is the Chern number, intuitively? For simplicity let's consider maps from S^2 to the non-degenerate two-band Hamiltonians described above. One picture is in terms of $\pi_2(S^2)$. An alternative picture is that a non-zero Chern number is an 'obstruction' to globally defining wavefunctions, in the following sense. F, the first Chern form, is a 2-form. Let's consider a constant non-zero F, which for the case $S^2 \to S^2$ can be viewed as the field of a monopole located at the centre of the target sphere. *Locally*, it is possible to find wavefunctions giving a vector potential A with $F = dA$, but not *globally*. (There has to be a 'Dirac string' passing through the surface of the sphere somewhere.) In other words, states with non-zero Chern number have Chern forms that are non-trivial elements of the second cohomology class: they are closed 2-forms that are not globally exact.

The one subtle thing about this two-band model is that there is a non-trivial invariant in *three* spatial dimensions, since $\pi_3(S^2) = \mathbb{Z}$ (the 'Hopf invariant'). In other words, even if the Chern numbers for the three 2D planes in this 3D structure are zero, there can still be an integer-valued invariant.[8] This map is familiar to physicists from the fact that the Pauli matrices can be used to map a normalized complex 2-component spinor, i.e. an element of S^3, to a real unit vector, i.e. an element of S^2: $n^i = \mathbf{z}^\dagger \sigma^i \mathbf{z}$. This 'Hopf map' is an example of a map that cannot be deformed to the trivial (constant) map. The Hopf invariant does not generalize naturally to more than two bands, but the Chern number does, as we now see.

Now we consider the case of a non-degenerate 2D band structure with multiple bands, which we study using a method of Avron, Seiler, and Simon [3]. By the same argument as in the two-band case, we would like to understand π_1 and π_2 of the target space $H_{n\times n}$, non-degenerate $n \times n$ Hermitian matrices. As before, we will find that π_1 is zero, so maps from T^2 are equivalent to maps from S^2, but the latter will be quite non-trivial. We first diagonalize H at each point in k-space:

$$H(k) = U(k)D(k)U^{-1}(k). \tag{1.55}$$

Here $U(k)$ is unitary and $D(k)$ is real diagonal and non-degenerate. We can smoothly distort D everywhere in the Brillouin zone to a reference matrix with eigenvalues $1, 2, \ldots$ because of the non-degeneracy: if we plot the jth eigenvalue of D as a function of k_x and k_y, then this distortion corresponds to smoothing out ripples in this plot to obtain a constant plane.

[8] The nature of this fourth invariant changes when the Chern numbers are non-zero, as shown by Pontryagin in 1941: it becomes an element of a finite group rather than of the integers.

The non-trivial topology is contained in $U(k)$. The key is to note that $U(k)$ in the above is ambiguous: right multiplication by any diagonal unitary matrix, an element of $DU(N)$, will give the same $H(k)$. So we need to understand the topology of $M = U(N)/DU(N) = SU(N)/SDU(N)$, where $SDU(N)$ means diagonal unitary matrices with determinant 1. We can compute π_2 of this quotient by using the exact sequence of a fibration and the following facts: $\pi_2(SU(N)) = \pi_1(SU(N)) = 0$ for $N \geq 2$. These imply that $\pi_2(M) \cong \pi_1(SDU(N)) = \mathbb{Z}^{n-1}$, i.e. $n-1$ copies of the integers. This follows from viewing $SDU(N)$ as N circles connected only by the requirement that the determinant be 1. Similarly, we obtain $\pi_1(M) = 0$. We interpret these $n-1$ integers that arise in homotopy theory as just the Chern numbers of the bands, together with a constraint that the Chern numbers sum to zero.

1.3.5 Time-reversal invariance in Fermi systems

Now we jump to 2004–2005, when it was noted that imposing time-reversal symmetry in 2D electronic systems leads to new topological invariants. While non-zero Chern numbers cannot be realized with time-reversal invariance, the zero-Chern-number class gets subdivided into two pieces: 'ordinary' insulators that do not in general have an edge state, and a QSHE or 'topological insulator' where a bulk topological invariant forces an edge state. The topological invariant is not an integer here but rather a two-valued or $\mathbb{Z}_2$ invariant.

The idea that triggered this development started from considering two copies of the quantum Hall effect, one for spin-up electrons and one for spin-down, with opposite effective magnetic fields for the two spins. This combination, studied early on by Murakami, Nagaosa, and Zhang [28], for example, is time-reversal-invariant because acting with the time-reversal operator T changes both the magnetic field direction and the spin. Note that in a model such as this, S_z is a conserved quantum number even though $SU(2)$ (spin-rotation invariance) is clearly broken, as up and down spins behave differently. Heuristically, think of the spin–orbit coupling as arising from intra-atomic terms like $\mathbf{L} \cdot \mathbf{S}$, and consider specifically $L_z S_z$. For an electron of fixed spin, this coupling to the orbital motion described by L_z is just like the coupling in a constant magnetic field, since the orbital motion L_z generates a magnetic dipole moment. In the simplest case of a Chern number $+1$ state of up electrons and a Chern number -1 state of down electrons, the edge will have counterpropagating modes: for example, up spin moves clockwise along the edge and down spin moves counterclockwise. This turns out to be not a bad caricature of the quantum spin Hall phase in a more realistic system: one can tell by symmetry arguments that it will have no quantum Hall effect (i.e. $\alpha_c = 0$ in $J_i = \alpha_c \epsilon_{ijk} E_j B_k$), but it will have a spin Hall effect

$$J^i_j = \alpha_s \epsilon_{ijk} E_k, \tag{1.56}$$

where α_c and α_s are some numerical constants and J^i_j is a spin current (a current of angular momentum i in spatial direction j.[9] The appearance of the electric field rather

[9] There are some challenges that arise in trying to define a spin current in a realistic physical system, chiefly because spin is not a conserved quantity. Spin currents are certainly real and measurable in

than the magnetic field in the quantum spin Hall equation results from the goal of having a potentially dissipationless current equation. If dissipation provides no 'arrow of time', then both sides should transform in the same way under the time-reversal operation, which fixes the field on the right side to be E rather than B.

As an example of this 'two copies of the IQHE' generated by spin–orbit coupling, consider the model of graphene introduced by Kane and Mele [19]. This is a tight-binding model for independent electrons on the honeycomb lattice (Fig. 1.1). The spin-independent part of the Hamiltonian consists of a nearest-neighbour hopping, which alone would give a semimetallic spectrum with Dirac nodes at certain points in the 2D Brillouin zone, plus a staggered sublattice potential whose effect is to introduce a gap:

$$H_0 = t \sum_{\langle ij \rangle \sigma} c^\dagger_{i\sigma} c_{j\sigma} + \lambda_v \sum_{i\sigma} \xi_i c^\dagger_{i\sigma} c_{i\sigma}. \tag{1.57}$$

Here $\langle ij \rangle$ denotes nearest-neighbour pairs of sites, σ is a spin index, ξ_i alternates sign between sublattices of the honeycomb, and t and λ_v are parameters.

The insulator created by increasing λ_v is an unremarkable band insulator. However, the symmetries of graphene also permit an 'intrinsic' spin–orbit coupling of the form

$$H_{SO} = i\lambda_{SO} \sum_{\langle\langle ij \rangle\rangle \sigma_1 \sigma_2} \nu_{ij} c^\dagger_{i\sigma_1} s^z_{\sigma_1\sigma_2} c_{j\sigma_2}. \tag{1.58}$$

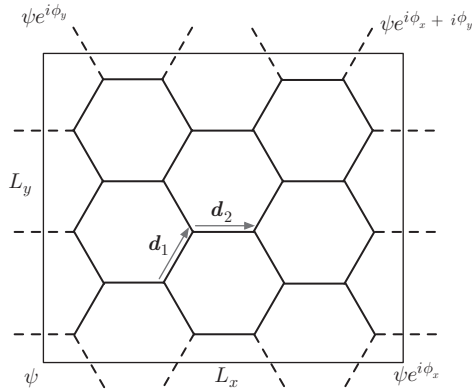

Fig. 1.1 The honeycomb lattice on which the tight-binding Hamiltonian resides. For the two sites depicted, the factor ν_{ij} of equation (1.58) is $\nu_{ij} = -1$. The phases $\phi_{x,y}$ describe twisted boundary conditions that are used in the text to give a pumping definition of the $\mathbb{Z}_2$ invariant. (Reprinted with permission from [9]. Copyright 2007 by the American Physical Society.)

various situations, but the fundamental definition we give of the quantum spin Hall phase will actually be in terms of charge; 'two-dimensional topological insulator' is another term for the same phase.

Here $\nu_{ij} = (2/\sqrt{3})\hat{\boldsymbol{d}}_1 \times \hat{\boldsymbol{d}}_2 = \pm 1$, where i and j are next-nearest neighbours and $\hat{\boldsymbol{d}}_1$ and $\hat{\boldsymbol{d}}_2$ are unit vectors along the two bonds that connect i to j. Including this type of spin–orbit coupling alone would not be a realistic model. For example, the Hamiltonian $H_0 + H_{SO}$ conserves s^z, the distinguished component of electron spin, and reduces for fixed spin (up or down) to Haldane's model [15]. Generic spin–orbit coupling in solids should not conserve any component of electron spin.

This model with S_z conservation is mathematically treatable using the Chern number above, since it just reduces to two copies of the IQHE. It is therefore not all that interesting, in addition to not being very physical, because of the requirement of S_z conservation. In particular, the stability of the phase is dependent on a subtle property of spin-$\frac{1}{2}$ particles (here we use the terms spin-$\frac{1}{2}$ and Fermi interchangeably). The surprise is that the quantum spin Hall phase survives, with interesting modifications, once we allow more realistic spin–orbit coupling, as long as time-reversal symmetry remains unbroken.

The time-reversal operator T acts differently in Fermi and Bose systems, or, more precisely, in half-integer versus integer spin systems. Kramers showed long ago that the square of the time-reversal operator is connected to a 2π rotation, which implies that

$$T^2 = (-1)^{2S}, \tag{1.59}$$

where S is the total spin quantum number of a state: half-integer-spin systems pick up a minus sign under two time-reversal operations.

An immediate consequence of this is the existence of 'Kramers pairs': every eigenstate of a time-reversal-invariant spin-$\frac{1}{2}$ system is at least twofold-degenerate. We will argue this perturbatively, by showing that a time-reversal-invariant perturbation H' cannot mix members of a Kramers pair (a state ψ and its time-reversal conjugate $\phi = T\psi$). To see this, note that

$$\langle T\psi|H'|\psi\rangle = \langle T\psi|H'|T^2\psi\rangle = -\langle T\psi|H'|\psi\rangle = 0, \tag{1.60}$$

where in the first step we have used the antiunitarity of T and the time-reversal symmetry of H' and in the second step the fact that $T^2 = -1$, while the last step is just to note that if $x = -x$, then $x = 0$.

Combining Kramers pairs with what is known about the edge state, we can say a bit about why a odd–even or $\mathbb{Z}_2$ invariant might be physical here. If there is only a single Kramers pair of edge states and we consider low-energy elastic scattering, then a right-moving excitation can only backscatter into its time-reversal conjugate, which is forbidden by the Kramers result above if the perturbation inducing scattering is time-reversal-invariant. However, if we have two Kramers pairs of edge modes, then a right-mover can backscatter to the left-mover that is *not* its time-reversal conjugate. This process will, in general, eliminate these two Kramers pairs from the low-energy theory.

Our general belief based on this argument is that a system with an even number of Kramers pairs will, under time-reversal-invariant backscattering, localize in pairs down to zero Kramers pairs, while a system with an odd number of Kramers pairs

will wind up with a single stable Kramers pair. Additional support for this odd–even argument will be provided by our next approach. We would like, rather than just trying to understand whether the edge is stable, to predict from bulk properties whether the edge will have an even or odd number of Kramers pairs. Since deriving the bulk–edge correspondence directly is quite difficult, what we will show is that, starting from the bulk T-invariant system, there are two topological classes. These correspond in the example above (of separated up and down spins) to paired IQHE states with even or odd Chern number for one spin. Then the known connection between Chern number and number of edge states is good evidence for the statements above about Kramers pairs of edge modes.

A direct Abelian Berry-phase approach for the 2D $\mathbb{Z}_2$ invariant is provided in Appendix 1.A, along with an introduction to Wess–Zumino (WZ) terms in $(1+1)$-dimensional field theory and a physical interpretation of the invariant in terms of pumping cycles. The common aspect between these two is that in both cases the 'physical' manifold (either the 2-sphere in the WZ case, or the 2-torus in the QSHE case) is extended in a certain way, with the proviso that the resulting physics must be independent of the precise nature of the extension. When we later go to 3D, it turns out that there is a very nice 3D non-Abelian Berry-phase expression for the 3D $\mathbb{Z}_2$ invariant; while in practice it is harder to compute than the original expression based on applying the 2D invariant, it is much more elegant mathematically, so we will focus on that. Actually, for practical calculations, a very important simplification for the case of inversion symmetry (in both $d = 2$ and $d = 3$) was made by Fu and Kane [12]: the topological invariant is determined by the product of eigenvalues of the inversion operator at the 2^d time-reversal-symmetric points of the Brillouin zone.

1.3.6 Experimental status of 2D insulating systems

This completes our discussion of 1D and 2D insulating systems. The 2D topological insulator was observed by a transport measurement in (Hg, Cd)Te quantum wells [21], following theoretical predictions [5]. A simplified description of this experiment is that it observed, in zero magnetic field, a two-terminal conductance $2e^2/h$, consistent with the expected conductance e^2/h for each edge if each edge has a single mode, with no spin degeneracy. More recent work has observed some of the predicted spin transport signatures as well, although, as expected, the amount of spin transported for a given applied voltage is not quantized, unlike the amount of charge.

In the next subsection, we start with the 3D topological insulator and its remarkable surface and magnetoelectric properties. We then turn to metallic systems in order to understand another consequence of Berry phases of Bloch electrons.

1.3.7 3D band structure invariants and topological insulators

We will give a very quick introduction to the band structure invariants that allowed generalization of the previous discussion of topological insulators to 3D. However, most of our discussion of the 3D topological insulator will be in terms of emergent properties that are difficult to perceive directly from the bulk band structure invariant. We start by asking to what extent the 2D IQHE can be generalized to 3D. A generalization of

the previous homotopy argument [3] can be used to show that there are three Chern numbers per band in 3D, associated with the xy, yz, and xz planes of the Brillouin zone. A more physical way to view this is that a 3D integer quantum Hall system consists of a single Chern number and a reciprocal lattice vector that describes the 'stacking' of integer quantum Hall layers. The edge of this 3D IQHE is quite interesting: it can form a 2D chiral metal, as the chiral modes from each IQHE combine and point in the same direction.

Consider the Brillouin zone of a 3D time-reversal-invariant material. Our approach will be to build on our understanding of the 2D case: concentrating on a single band pair, there is a $\mathbb{Z}_2$ topological invariant defined in the 2D problem with time-reversal invariance. Taking the Brillouin zone to be a torus, there are two inequivalent xy planes that are distinguished from others by the way time-reversal acts: the $k_z = 0$ and $k_z = \pm\pi/a$ planes are taken to themselves by time reversal (note that $\pm\pi/a$ are equivalent because of the periodic boundary conditions). These special planes are essentially copies of the 2D problem, and we can label them by $\mathbb{Z}_2$ invariants $z_0 = \pm 1$, $z_{\pm 1} = \pm 1$, where $+1$ denotes 'even Chern parity' or ordinary 2D insulator and -1 denotes 'odd Chern parity' or topological 2D insulator. Other xy planes are not constrained by time reversal and hence do not have to have a $\mathbb{Z}_2$ invariant.

The most interesting 3D topological insulator phase (the 'strong topological insulator') results when the z_0 and $z_{\pm 1}$ planes are in different 2D classes. This can occur if, moving in the z direction between these two planes, one has a series of 2D problems that interpolate between ordinary and topological insulators by breaking time reversal invariance. We will concentrate on this type of 3D topological insulator here. Another way to make a 3D topological insulator is to stack 2D topological insulators, but considering the edge of such a system shows that it will not be very stable: since two 'odd' edges combine to make an 'even' edge, which is unstable in the presence of T-invariant backscattering, we call such a stacked system a 'weak topological insulator'.

Above we found two xy planes with 2D $\mathbb{Z}_2$ invariants. By the same logic, we could identify four other such invariants: x_0, $x_{\pm 1}$, y_0, $y_{\pm 1}$. However, not all six of these invariants are independent: some geometry (an exercise for the reader) shows that there are two relations, reducing the number of independent invariants to four:[10]

$$x_0 x_{\pm 1} = y_0 y_{\pm 1} = z_0 z_{\pm 1}. \tag{1.61}$$

We can take these four invariants in 3D as $(x_0, y_0, z_0, x_0 x_{\pm 1})$, where the first three describe layered 'weak' topological insulators and the last describes the genuinely 3D invariant that distinguishes 'strong' topological insulators. (Note that one material can hence be both a strong and a weak topological insulator by this definition.)

[10] *Sketch of geometry:* To establish the first of these equalities, consider evaluating the Fu-Kane 2D formula on the four effective Brillouin zones (EBZs, see Section 1.A.2) described by the four invariants x_0, x_{+1}, y_0, y_{+1}. These define a torus, on whose interior the Chern 2-form F is well defined. Arranging the four invariants so that all have the same orientation, the A terms drop out, and the F integral vanishes since the torus can be shrunk to a loop. In other words, for some gauge choice, the difference $x_0 - x_{+1}$ is equal to $y_0 - y_{+1}$.

Alternatively, the 'axion electrodynamics' field theory in the next subsection can be viewed as suggesting that there should be only one genuinely 3D $\mathbb{Z}_2$ invariant.

For example, the strong topological insulator cannot be realized in any model with S_z conservation, while, as explained earlier, a useful example of the 2D topological insulator (a.k.a. QSHE) can be obtained from combining IQHE phases of up and down electrons. The impossibility of making a strong topological insulator with S_z conservation follows from noting that all planes normal to z have the same Chern number, since the Chern number is a topological invariant whether or not the plane is preserved by time- reversal. In particular, the $k_z = 0$ and $k_z = \pm\pi/a$ phases have the same Chern number for up electrons, say, which means that these two planes are either both 2D ordinary or both 2D topological insulators.

While the above argument is valid and useful for connecting the 3D topological insulators to the 2D case, it doesn't give much insight into what sort of gapless surface states we should expect at the surface of a strong topological insulator. The answer can be obtained by other means (some properties can be found via the field-theory approach given in the next section): the spin-resolved Fermi surface encloses an odd number of Dirac points. In the simplest case of a single Dirac point, believed to be realized in Bi_2Se_3, the surface state can be pictured as 'one-quarter of graphene'. Graphene, a single layer of carbon atoms that form a honeycomb lattice, has two Dirac points and two spin states at each k; spin–orbit coupling is quite weak, since carbon is a relatively light element. The surface state of a 3D topological insulator can have a single Dirac point and a single spin state at each k. As in the edge of the 2D topological insulator, time-reversal invariance implies that the spin state at k must be the T conjugate of the spin state at $-k$.

1.3.8 Axion electrodynamics, second Chern number, and magnetoelectric polarizability

The 3D topological insulator turns out to be connected to a basic electromagnetic property of solids. We know that in an insulating solid, Maxwell's equations can be modified because the dielectric constant ϵ and magnetic permeability μ need not take their vacuum values. Another effect is that solids can generate the electromagnetic term

$$\Delta\mathcal{L}_{EM} = \frac{\theta e^2}{2\pi h}\mathbf{E}\cdot\mathbf{B} = \frac{\theta e^2}{16\pi h}\epsilon^{\alpha\beta\gamma\delta}F_{\alpha\beta}F_{\gamma\delta}. \tag{1.62}$$

This term describes a magnetoelectric polarizability: an applied electrical field generates a magnetic dipole, and vice versa. An essential feature of the above 'axion electrodynamics' theory (cf. Wilczek [42]) is that when the axion field $\theta(\boldsymbol{x}, t)$ is constant, it plays no role in electrodynamics; this follows because θ couples to a total derivative, $\epsilon^{\alpha\beta\gamma\delta}F_{\alpha\beta}F_{\gamma\delta} = 2\epsilon^{\alpha\beta\gamma\delta}\partial_\alpha(A_\beta F_{\gamma\delta})$ (here we have used that F is closed, i.e. $dF = 0$), and so does not modify the equations of motion. However, the presence of the axion field can have profound consequences at surfaces and interfaces, where gradients in $\theta(\mathbf{x})$ appear.

A bit of work shows that at a surface where θ changes, there is a surface quantum Hall layer of magnitude

$$\sigma_{xy} = \frac{e^2(\Delta\theta)}{2\pi h}. \tag{1.63}$$

(This can be obtained by moving the derivative from one of the A fields to act on θ, leading to a Chern–Simons term for the electromagnetic field at the surface. The connection between Chern–Simons terms and the quantum Hall effect will be a major subject of the last part of this chapter.) The magnetoelectric polarizability described above can be obtained from these layers: for example, an applied electric field generates circulating surface currents, which in turn generate a magnetic dipole moment. In a sense, σ_{xy} is what accumulates at surfaces because of the magnetoelectric polarizability, in the same way as charge is what accumulates at surfaces because of ordinary polarization.

We are jumping ahead a bit in writing θ as an angle: we will see that, like polarization, θ is only well defined as a bulk property modulo 2π (for an alternative picture showing why θ is periodic that is more appropriate for electroweak symmetry breaking, see [42]). The integer multiple of 2π is only specified once we specify a particular way to make the boundary. How does this connect to the 3D topological insulator? At first glance, $\theta = 0$ in any time-reversal-invariant system, since $\theta \to -\theta$ under time reversal. However, as θ is periodic, $\theta = \pi$ also works, since $-\theta$ and θ are equivalent because of the periodicity, and is inequivalent to $\theta = 0$.

Here we will not give a microscopic derivation of how θ includes, for a band structure of non-interacting electrons, a part that is an integral of the Chern–Simons form:

$$\theta = \frac{1}{2\pi}\int_{\mathrm{BZ}} d^3k\, \epsilon_{ijk}\, \mathrm{Tr}\left[\mathcal{A}_i\partial_j\mathcal{A}_k - i\frac{2}{3}\mathcal{A}_i\mathcal{A}_j\mathcal{A}_k\right], \tag{1.64}$$

which can be done by imitating our previous derivation of the polarization formula [10, 34]. In general, unlike for the electrical polarization, there are additional non-geometrical contributions as well [11, 24]. Instead, we will focus on understanding the physical and mathematical meaning of the Chern–Simons form that constitutes the integrand, chiefly by discussing analogies with our previous treatment of polarization in 1D and the IQHE in 2D. These analogies are summarized in Table 1.1.

Throughout this subsection,

$$\mathcal{F}_{ij} = \partial_i\mathcal{A}_j - \partial_j\mathcal{A}_i - i[\mathcal{A}_i, \mathcal{A}_j] \tag{1.65}$$

is the (generally non-Abelian) Berry curvature tensor ($\mathcal{A}_\lambda = i\langle u|\partial_\lambda|u\rangle$), and the trace and commutator refer to band indices. We can gain an understanding of the above Chern–Simons form $K = \mathrm{Tr}[\mathcal{A}_i\partial_j\mathcal{A}_k - i\frac{2}{3}\mathcal{A}_i\mathcal{A}_j\mathcal{A}_k]$ by starting from the second Chern form $\mathrm{Tr}[\mathcal{F}\wedge\mathcal{F}]$; the relationship between the two is

$$dK = \mathrm{Tr}[\mathcal{F}\wedge\mathcal{F}], \tag{1.66}$$

Table 1.1 Comparison of Berry-phase theories of polarization and magnetoelectric polarizability

	POLARIZATION	MAGNETOELECTRIC POLARIZABILITY
$d_{\min}$	1	3
Observable	$\mathbf{P} = \dfrac{\partial \langle H \rangle}{\partial E}$	$M_{ij} = \dfrac{\partial \langle H \rangle}{\partial E_i \, \partial B_j} = \dfrac{\delta_{ij} \theta e^2}{2\pi h}$
Quantum	$\Delta \mathbf{P} = \dfrac{e\mathbf{R}}{\Omega}$	$\Delta M = \dfrac{e^2}{h}$
Surface	$q = (\mathbf{P}_1 - \mathbf{P}_2) \cdot \hat{\mathbf{n}}$	$\sigma_{xy} = M_1 - M_2$
Electromagnetic coupling	$\mathbf{P} \cdot \mathbf{E}$	$M \mathbf{E} \cdot \mathbf{B}$
Chern–Simons form	$\mathcal{A}_i$	$\epsilon_{ijk} \left(\mathcal{A}_i \mathcal{F}_{jk} + i \frac{1}{3} \mathcal{A}_i \mathcal{A}_j \mathcal{A}_k \right)$
Chern form	$\epsilon_{ij} \partial_i \mathcal{A}_j$	$\epsilon_{ijkl} \mathcal{F}_{ij} \mathcal{F}_{kl}$

just as $\mathcal{A}$ is related to the first Chern form: $d(\operatorname{Tr} \mathcal{A}) = \operatorname{Tr} \mathcal{F}$. These relationships hold locally (this is known as Poincaré's lemma—that, given a closed form, it is *locally* an exact form) but not globally, unless the first or second Chern form generates the trivial cohomology class. For example, we saw that the existence of a non-zero first Chern number on the sphere prevented us from finding globally defined wavefunctions that would give an $\mathcal{A}$ with $d\mathcal{A} = \mathcal{F}$. We are assuming in even writing the Chern–Simons formula for θ that the ordinary Chern numbers are zero, so that an $\mathcal{A}$ can be defined in the 3D Brillouin zone. We would run into trouble if we assumed that an $\mathcal{A}$ could be defined in the 4D Brillouin zone if the *first or second* Chern number were non-zero. Note that the electromagnetic action above is just the second Chern form of the (Abelian) electromagnetic field.

The second Chern form is closed and hence generates an element of the de Rham cohomology we studied earlier. There are higher Chern forms as well: the key is that symmetric polynomials can be used to construct closed forms, by the antisymmetry properties of the exterior derivative. In physics, we typically keep the manifold fixed (in our Brillouin zone examples, it is usually a torus T^n), and are interested in classifying different fibre bundles on the manifold. In mathematical language, we want to use a properly normalized cohomology form to compute a homotopy invariant (i.e. with respect to changing the connection, not the manifold). This is exactly what we did with the Chern number in the IQHE, which was argued to compute certain integer-valued homotopy π_2 invariants of non-degenerate Hermitian matrices.

More precisely, we saw that the $U(1)$ gauge dependence of polarization was connected to the homotopy group $\pi_1(U(1)) = \mathbb{Z}$, but that this is connected also to the existence of integer-valued Chern numbers, which we explained in terms of π_2. (These statements are not as inconsistent as they might seem, because our calculation of

π_2 came down to π_1 of the diagonal unitary group.) We can understand the second Chern and Chern–Simons form similarly, using the homotopy invariants π_3 (gauge transformation in $d = 3$) and π_4 (quantized state in $d = 4$). The Chern–Simons integral for θ given above, in the non-Abelian case, has a $2\pi n$ ambiguity under gauge transformations, and this ambiguity counts the integer-valued homotopy invariant

$$\pi_3(SU(N)) = \mathbb{Z}, \quad N \geq 2. \tag{1.67}$$

In other words, there are 'large' (non-null-homotopic) gauge transformations. Note that the Abelian Chern–Simons integral is completely gauge-invariant, consistent with $\pi_3(U(1)) = 0$.

The quantized state in $d = 4$ was originally discussed in the context of time-reversal-symmetric systems. The set $\mathcal{Q}$ has one integer-valued π_4 invariant for each band pair, with a zero-sum rule. These invariants survive even once T is broken, but realizing the non-zero value requires that two bands touch somewhere in the 4D Brillouin zone. In this sense, the '4D quantum Hall effect' is a property of how pairs of bands interact with each other, rather than of individual bands. Even if this 4D QHE is not directly measurable, it is mathematically connected to the 3D magnetoelectric polarizability in the same way as 1D polarization and the 2D IQHE are connected.

The above Chern–Simons formula for θ works, in general, only for a non-interacting electron system. This is not true for the first Chern formula for the IQHE, or the polarization formula, so what is different here? The key is to remember that the 3D Chern formula behaves very differently in the Abelian and non-Abelian cases; for example, in the Abelian case, θ is no longer periodic as the integral is fully gauge-invariant. Taking the ground state many-body wavefunction and inserting it into the Chern–Simons formula is not guaranteed to give the same result as using the multiple one-particle wavefunctions.

However, we can give a many-body understanding of θ that clarifies the geometric reason for its periodicity even in a many-particle system. Consider evaluating dP/dB by applying the 3D polarization formula

$$P_i = e \int_{BZ} \frac{d^3k}{(2\pi)^3} \operatorname{Tr} \mathcal{A}_i \,. \tag{1.68}$$

to a rectangular-prism unit cell. The minimum magnetic field normal to one of the faces that can be applied to the cell without destroying the periodicity is one flux quantum per unit cell, or a field strength $h/(e\Omega)$, where Ω is the area of that face. The ambiguity of polarization (1.68) in this direction is one charge per transverse unit cell area, i.e. e/Ω. Then the ambiguity in dP/dB is

$$\Delta \frac{P_x}{B_x} = \frac{e/\Omega}{h/(e\Omega)} = \frac{e^2}{h} = 2\pi \frac{e^2}{2\pi h}. \tag{1.69}$$

So the periodicity of 2π in θ is really a consequence of the geometry of polarization, and is independent of the single-electron assumption that leads to the microscopic Chern–Simons formula.

1.3.9 Anomalous Hall effect and Karplus–Luttinger anomalous velocity

Our previous examples of Berry phases in solids have concentrated on insulators, but one of the most direct probes of the Berry phase of Bloch electrons is found in metals that break time-reversal symmetry. The breaking of T allows a non-zero transverse conductivity σ_{xy} to exist along with the metallic diagonal conductivity σ_{xx}. This 'anomalous Hall effect' (AHE) can originate from several different microscopic processes. The most interesting from a geometric point of view is the intrinsic AHE that results from Berry phases of a time-reversal-breaking band structure when the Fermi level is in the middle of a band. We will not attempt to discuss this interesting physics here but refer the reader to a comprehensive review by Nagaosa et al. [29] and note that there are an increasing number of other examples of Berry-phase effects in metals. There are similar effects related to the orbital moment of Bloch electrons, which is similar in some ways but not purely geometric since it arises from both the wavefunctions and the Hamiltonian, unlike the Berry phase, which is purely a wavefunction property.

1.4 Introduction to topological order

Now we consider strongly interacting topological phases, defined as those that cannot be understood in terms of free particles. In contrast, the IQHE and topological insulators can be understood in terms of free particles, although these phases are stable in the sense that they survive over a finite region of interaction strength until a phase transition occurs. Our main tool will be quantum field theory, which is a powerful language to describe the long-wavelength physics of interacting systems. After giving some microscopic motivation from the fractional quantum Hall effect (FQHE), we give a first example of field theory applied to spin chains as an example of how an analysis of topological terms in a simple field theory led to a clear experimental prediction (the 'Haldane gap') regarding antiferromagnetic integer-spin Heisenberg chains.

We then return to the quantum Hall effect and develop Abelian Chern–Simons theory, an example of a truly topological field theory. Although it is written in terms of one or more $U(1)$ gauge fields, similar to ordinary electromagnetism, its behaviour is strikingly different from that of the conventional field theories with which the reader may already be familiar. In lieu of a microscopic derivation, which has been carried out but is somewhat tedious, we show that it unifies properties such as ground-state degeneracy, braiding statistics, and edge excitations. We will follow increasingly standard parlance and use the term 'topological order' specifically for phases of matter described by a non-trivial topological field theory, hence having ground-state degeneracy, fractional statistics, etc. Thus the IQHE, which is certainly a topological phase of matter and well described by the Abelian Chern–Simons theory given below with $k = 1$, does not have topological order in the sense introduced by Wen.

1.4.1 FQHE background

We give quickly some standard background on the FQHE in order to motivate the Chern–Simons field theory introduced below. The goal of that field theory is to give a

compact universal description of the key features of the topological order in quantum Hall states, similar in spirit to the Ginzburg–Landau field theory of symmetry-breaking phases. Most of this material is standard and can be found in a number of edited volumes and textbooks on the quantum Hall effects [6, 18, 33].

Our discussion centres on the Laughlin wavefunction for 2D electrons ($z_j = x_j + iy_j$ describes the jth electron, $j = 1, \ldots, N$)

$$\Psi_m = \left[\prod_{i<j}(z_i - z_j)^m\right] \exp\left(-\sum_i |z_i|^2/4\ell^2\right). \tag{1.70}$$

The magnetic length is $\ell = \sqrt{\hbar c/eB}$ and the wavefunction is not normalized. This wavefunction clearly can be expanded over the single-electron lowest-Landau-level wavefunctions in the rotational gauge,

$$\psi_m = z^m e^{-|z|^2/4\ell^2}. \tag{1.71}$$

where $m = 0, 1, \ldots$ labels angular momentum. For $m = 1$, the Laughlin state is just a Slater determinant for the filled lowest Landau level, but for higher m, it is believed not to be a sum of any finite number of Slater determinants in the $N \to \infty$ limit.

This wavefunction can be justified using the pseudopotential approach introduced by Haldane: it is the maximum-density zero-energy state of a repulsive interaction that vanishes for relative angular momentum greater than or equal to m. We checked that its density is $\nu = 1/m$ by looking at the degree of the polynomial factor, which is directly related to $\langle r^2 \rangle$, and argued that it contains 'quasihole' excitations of charge $-q/m$, where q is the charge of the electrons. The wavefunction for a quasihole at z_0 is

$$\Psi_{\text{quasihole}} = \left[\prod_i (z_i - z_0)\right] \Psi_m. \tag{1.72}$$

The fractional charge can be understood by noting that m copies of the extra factor here would lead to a wavefunction with an electron at z_0, but without treating z_0 as an electron coordinate; in other words, a wavefunction with a 'hole' added at z_0. It has edge states that at first glance are loosely similar to those in the filled Landau level.

1.4.2 Topological terms in field theories: the Haldane gap and Wess–Zumino–Witten models

As a warm-up for fully topological field theories, we give an example of how topological terms can have profound consequences in 'ordinary' field theories (i.e. theories without gauge fields). By a topological term, we mean loosely one whose value in any specific configuration (a path in the path integral) is a topological invariant, so that the set of all paths can be divided into topological sectors by the value of the topological term. A famous example of this phenomenon found by Haldane led to the first understanding of the gapped spin-1 Heisenberg antiferromagnet in one spatial

dimension, which has recently been interpreted as a symmetry-protected topological phase of interacting particles because it can be smoothly connected to a trivial phase by breaking spatial symmetries such as inversion. We will focus on topological terms that appear in nonlinear σ-models, which, despite their unwieldy name, are a very basic type of field theory for systems in or near an ordered phase breaking a continuous symmetry.

We first present Haldane's example (following closely the treatment of Auerbach [2]), and then discuss a different kind of topological term that appears in Wess–Zumino–Witten models, again in one spatial dimension; details of the latter are provided in Appendix 1.A. The nonlinear σ-model (NLSM) is an example of an effective theory, a simplified description of the low-energy degrees of freedom of a complicated system. Ginzburg–Landau theory is another such effective theory, and one use of the NLSM is as a further simplification of Ginzburg–Landau theory where we have thrown away the 'hard' or 'massive' fluctuations of the magnitude of the order parameter, keeping only the 'soft' or 'massless' fluctuations within the order-parameter manifold.

For definiteness, we consider a d-dimensional XY model, which would be described in Ginzburg–Landau theory by a 2-component real or 1-component complex order parameter. The mean-field physics in the ordered phase as a function of the order parameter is as follows: the order-parameter manifold of symmetry-related ground states is a circle, and we can expect that fluctuations along this circle are 'soft' in the sense of requiring little energy (since this is a flat direction of the energy), while those perpendicular to the circle are more costly. This order-parameter manifold is the same as that considered in the discussion of topological defects in Section 1.2, where defects were classified using maps from surfaces enclosing the defect in real space to the order-parameter manifold. At low temperature, we might expect that a reasonable description of the system is therefore obtained just from fluctuations of the order parameter's direction, leading to a functional integral for the coarse-grained classical partition function:

$$Z_{\mathrm{NLSM}} = \int \mathcal{D}\theta(x) \exp\left[-\beta c \int \frac{(\nabla\theta)^2}{2}\, d^d x\right]. \tag{1.73}$$

Here c is a coupling constant with units of energy if $d = 2$; one could estimate c simply from the coupling strength in a lattice XY model. The NLSM it is called nonlinear because the circle is defined by a hard constraint on the $\hat{\mathbf{n}}$ field, which in more complicated target manifolds such as the sphere leads to interaction (i.e. nonlinear) terms in the fields obtained in a perturbative expansion; it is called a σ-model because of its first appearance in particle physics.

For a quantum-mechanical model at zero temperature, we might expect on general grounds that imaginary time will become an extra dimension in any Euclidean path-integral representation of the partition function, in the same way as the Dirac–Feynman path integral for quantum mechanics involves integration of the Lagrangian over time (a $(0+1)$-dimensional theory). Now we will obtain a NLSM for

a quantum-mechanical problem in one spatial dimension. Heuristically, we might expect an NLSM to be a reasonable description for a quantum model that is 'close to' having symmetry-breaking order.

Our approach is to derive a connection between the low-energy, long-wavelength degrees of freedom of the spin path integral of the Heisenberg antiferromagnet. This process is known as Haldane's mapping in the context of spin systems: we will use it to show that there is a topological term present for half-integer spin but not for integer spin, which is believed to explain the different behaviour seen numerically and experimentally in these two cases.

First we look for a more general way of writing the Berry -phase term for a spin that results from setting up a coherent-state path integral for spin. In order to make a path integral, we should set up an integral over 'classical' trajectories—what is the classical trajectory of a spin? One answer is to use the overcomplete basis of coherent states for the spin-S Hilbert space [2], which are labelled by a unit vector $\hat{\mathbf{\Omega}}$. As S increases, the spin wavefunction becomes more and more concentrated around $\hat{\mathbf{\Omega}}$:

$$\omega[\hat{\mathbf{\Omega}}] = -\int_0^\beta d\tau \dot{\phi} \cos\theta. \tag{1.74}$$

For a closed path on the sphere, this corresponds to the signed spherical area enclosed by the path. An overall ambiguity of $\pm 4\pi$ in this area does not affect the physics, since the area ω appears in the path-integral action with a coefficient $-iS$. For a many-spin system, the full action is

$$S[\hat{\mathbf{\Omega}}] = -iS \sum_i \omega[\hat{\mathbf{\Omega}}_i] + \int_0^\beta d\tau \, \frac{S^2 J}{2} \sum_{ij} \hat{\mathbf{\Omega}}_i \cdot \hat{\mathbf{\Omega}}_j. \tag{1.75}$$

For now, we return to a single spin to set up an improved way of writing the Berry-phase term.

Let the vector potential $\mathbf{A}(\hat{\mathbf{\Omega}})$ be assumed to have the property that its line integral over a closed orbit on the sphere should give the area enclosed by the orbit:

$$\omega = \int_0^\beta d\tau \, \mathbf{A}(\hat{\mathbf{\Omega}}) \cdot \dot{\hat{\mathbf{\Omega}}}. \tag{1.76}$$

Then Stokes's theorem fixes curl $\mathbf{A}$ to be the magnetic field of a magnetic monopole (a vector with uniform outward component):

$$\nabla \times \mathbf{A} \cdot \hat{\mathbf{\Omega}} = \epsilon^{\alpha\beta\gamma} \frac{\partial A_\beta}{\partial \hat{\Omega}_\alpha} \hat{\Omega}^\gamma = 1. \tag{1.77}$$

Two explicit examples to check that this can be done are

$$\mathbf{A}^a = -\frac{\cos\theta}{\sin\theta}\hat{\phi}, \qquad \mathbf{A}^b = \frac{1-\cos\theta}{\sin\theta}\hat{\phi}. \tag{1.78}$$